

See discussions, stats, and author profiles for this publication at: <https://www.researchgate.net/publication/41187747>

Thermochemical Properties and Electronic Structure of Boron Oxides B_nOm ($n=5-10$, $m=1-2$) and Their Anions

ARTICLE in THE JOURNAL OF PHYSICAL CHEMISTRY A · MARCH 2010

Impact Factor: 2.69 · DOI: 10.1021/jp909512m · Source: PubMed

CITATIONS

24

READS

32

3 AUTHORS:



Truong Tai

University of Leuven

65 PUBLICATIONS 506 CITATIONS

[SEE PROFILE](#)



Minh Tho Nguyen

University of Leuven

748 PUBLICATIONS 10,835 CITATIONS

[SEE PROFILE](#)



David A Dixon

University of Alabama

766 PUBLICATIONS 22,167 CITATIONS

[SEE PROFILE](#)

Thermochemical Properties and Electronic Structure of Boron Oxides B_nO_m ($n = 5–10$, $m = 1–2$) and Their Anions

Truong Ba Tai,[†] Minh Tho Nguyen,^{*,†,‡} and David A. Dixon^{*,‡}

Department of Chemistry and LMCC-Mathematical Modeling and Computational Science Center, Katholieke Universiteit Leuven, B-3001 Leuven, Belgium, and Department of Chemistry, The University of Alabama, Shelby Hall, Box 870336, Tuscaloosa, Alabama 35847-0336

Received: October 4, 2009; Revised Manuscript Received: December 6, 2009

The molecular and electronic structures of a series of small boron monoxide and dioxide clusters B_nO_m ($n = 5–10$, $m = 1, 2$) plus their anions were predicted. The enthalpies of formation (ΔH_f 's), electron affinities (EAs), vertical detachment energies, and energies of different fragmentation processes are predicted using the G3B3 method. The G3B3 results were benchmarked with respect to more accurate CCSD(T)/CBS values for $n = 1–4$ with average deviations of ± 1.5 kcal/mol for ΔH_f 's and ± 0.03 eV for EAs. The results extend previous observations on the growth mechanism for boron oxide clusters: (i) The low spin electronic state is consistently favored. (ii) The most stable structure of a neutral boron monoxide B_nO is obtained either by condensing O on a BB edge of a B_n cycle, or by binding one BO group to a B_{n-1} ring. The balance between both factors is dependent on the inherent stability of the boron cycles. (iii) A boron dioxide is formed by incorporating the second O atom into the corresponding monoxide to form BO bonds. (iv) A $B_nO_m^-$ anion is constructed with BO groups bound to the B_{n-1} or B_{n-2} rings (yielding the $B_{n-2}(BO)_2^-$ species). This becomes the preferred geometry for the larger boron dioxides, even in the neutral state. The boronyl group mainly behaves as an electron-withdrawing substituent reducing the binding energy and resonance energy of the oxides. (v) The boron oxides conserve some of the properties of the parent boron clusters such as the planarity and multiple aromaticity.

Introduction

Boron and boron-based clusters have attracted much attention due to their interesting physical and chemical properties.^{1–4} Boron's small covalent radius and the strong bonds that it can form with oxygen have led to the consideration of boron oxides for superhard⁵ materials. A number of studies on the molecular and electronic structures and the spectroscopic and thermochemical properties of small boron oxide clusters have been reported. Anderson and co-workers¹ experimentally investigated the oxidation of boron clusters and the subsequent reactions of the $B_nO_m^+$ cations with small molecules in the gas phase. Wang and co-workers⁶ used experimental photoelectron spectroscopy coupled with quantum chemical calculations to probe the electronic structures of small anions including $B_3O_2^-$, $B_4O_2^-$, $B_4O_3^-$, and $B_4O_2^{2-}$ and their neutral counterparts. Most of the theoretical studies have focused on B_nO_m species with n as large as 5.^{7–23} Recently, we predicted the enthalpies of formation and determined the electronic structures of a series of small B_nO_m compounds and their anions with $n = 1–4$ and $m = 1–3$ using high accuracy computational methods at the coupled-cluster theory CCSD(T) level with the correlation consistent aug-cc-pVnZ ($n = D, T, Q, 5$) basis sets extrapolated to the complete basis set limits (CBS) with additional corrections.²³ The calculated detachment energies are in good agreement with the available experimental data. In addition, we discussed the main factors governing the growth mechanism, geometries, and electronic structures of these small boron oxides.²³

Only a few studies on B_nO_m containing a number of $n > 5$ have been reported. Drummond et al.²⁴ predicted the molecular structures and stabilities of the B_nO_m neutrals with $n = 1–9$ and $m = 1–3$ from molecular dynamics simulation techniques in conjunction with plane-wave density functional theory (DFT) with the PW91 functional. Feng et al.²⁵ reported a DFT study with the B3LYP functional of both monoxides B_nO and dioxides B_nO_2 for $n = 1–6$. In view of the lack of reliable data on boron oxides, we have extended our computational efforts to a systematic investigation of the electronic structures, thermodynamic stabilities, and growth mechanisms of B_nO_m compounds with $n = 5–10$ and $m = 1–2$ and the corresponding anions. The thermochemical properties including the heats of formation, vertical (VDE) and adiabatic (ADE) detachment energies, and binding energies are determined using the composite G3B3 method.²⁶ The G3B3 method was used to calculate the properties for the smaller B_nO_m species with $n = 1–4$, and the results were benchmarked against the values obtained in our previous study using the CCSD(T)/CBS approach.²³ To better understand the nature of chemical bonding in these boron oxides, the topology of the electron localization function (ELF)²⁷ was calculated using B3LYP/6-311G(d) densities.

Computational Methods

All quantum chemical calculations were carried out using the Gaussian 03²⁸ suite of programs. Total atomization energies (TAEs) were calculated using the G3B3 approach.²⁹ By combining the calculated TAE values with the known heats of formation at 0 K for the elements, $\Delta H_f^\circ(B) = 135.1 \pm 0.2$ kcal/mol³⁰ and $\Delta H_f^\circ(O) = 58.98 \pm 0.02$ kcal/mol,³¹ the ΔH_f° values at 0 K of the B_nO_m species can be evaluated. A rationale for

* Corresponding authors. E-mail: minh.nguyen@chem.kuleuven.be (M.T.H.); dadixon@as.ua.edu (D.A.D.).

[†] Katholieke Universiteit Leuven.

[‡] The University of Alabama.

TABLE 1: Calculated Heats of Formation (ΔH_f , kcal/mol) for the Boron Oxides B_nO_m ($n = 1–4$, $m = 1–2$) at the G3B3 and CCSD(T)/CBS levels

structure	symmetry, state	$\Delta H_f(0\text{ K})$		$\Delta H_f(298\text{ K})$	
		G3B3	CBS ^a	G3B3	CBS ^a
BO	$C_{\infty h}, ^2\Sigma^+$	2.2	1.7	2.9	2.4
BO^-	$C_{\infty h}, ^1\Sigma^+$	-57.1	-56.1	-56.4	-55.3
OB ₂	$D_{\infty h}, ^2\Pi_g$	-66.7	-66.0	-66.6	-65.9
BO_2^-	$D_{\infty h}, ^1\Sigma_g^+$	-169.9	-169.4	-170.0	-169.5
BOB	$D_{\infty h}, ^1\Sigma_g^+$	40.8	40.9	42.1	41.7
BOB^-	$D_{\infty h}, ^2\Sigma_g^+$	38.5	39.2	39.6	40.5
BBO	$C_{\infty h}, ^1\Sigma^+$	56.3	57.2	57.6	58.4
BBO^-	$C_{\infty h}, ^2\Pi$	22.5	24.1 ^b	23.6	25.1 ^b
OBBO	$D_{\infty h}, ^1\Sigma_g^+$	-110.1	-109.8	-109.5	-109.4
OBBO ⁻	$C_{2h}, ^2B_u$	-118.7	-118.4	-118.0	-117.6
B ₃ O	$C_{\infty h}, ^4\Sigma^-$	97.8	98.0	99.2	99.3
B ₃ O ⁻	$C_{2v}, ^3A_1$	46.4	50.6	47.8	51.8
B ₃ O ₂	$D_{\infty h}, ^2\Pi_g$	-39.1	-38.8	-38.0	-38.4
B ₃ O ₂ ⁻	$D_{\infty h}, ^3\Sigma_u^-$	-107.7	-106.5	-106.6	-105.5
B ₄ O	$C_{2v}, ^1A_1$	111.3	112.7	112.8	114.2
B ₄ O ⁻	$C_{2v}, ^2A_1$	48.4	53.3	49.8	54.7
B ₄ O ₂	$D_{\infty h}, ^3\Sigma_g^-$	-9.4	-8.1	-8.0	-6.6
B ₄ O ₂ ⁻	$D_{\infty h}, ^2\Pi$	-82.6	-80.4	-81.2	-79.0

^a CCSD(T)/CBS values from ref 23. ^b CCSD(T)/CBS values, this work.

the choice of the heat of formation for the boron atom has been given previously.^{23,32} The heats of formation at 298 K are derived by adding the corresponding thermal corrections.³³ In the G3B3 approach, the equilibrium geometries and vibrational frequencies are calculated at the B3LYP/6-31G(d) level.^{34–36} The ELF²⁷ plots are supplemented by a determination of their topological bifurcations.³⁷ The ELF is a local measure of the Pauli repulsion between electrons due to the exclusion principle in three-dimensional space. Such a localization technique allows the partition of the total density into basins, which correspond to the molecular regions containing the cores, lone pairs, and chemical bonds. The total ELFs are mapped out using the TOPMOD software,³⁸ and all ELF isosurfaces are plotted using the OpenMol software.³⁹ The natural bond orbitals (NBOs)^{40–42} are constructed using the B3LYP/6-311+G(d) densities.

Results and Discussion

The G3B3 enthalpies of formation at 0 and 298 K for neutral and anionic B_nO_m with $n = 1–4$ are summarized in Table 1, together with the previous CCSD(T)/CBS values.²³ Figure 1 displays the lowest-lying structure of the neutral compounds for $n = 1–4$ to facilitate comparison with the larger structures. The energetically lowest-lying isomeric structures of the larger species B_nO_m , with $n = 5–10$ and $m = 1–2$, and their anions are shown in Figures 2–7. A number of structures were constructed and optimized based on our analysis of the structures of the smaller boron oxides²³ and the structures of the larger bare boron clusters and their anions.⁴³ Structures of the neutrals and corresponding anions are labeled $B_nO_m\text{-X}$ (neutrals) and $B_nO_m\text{-X}^-$ (anions) with X = A, B, C, When X is the same, both the neutral and anionic forms have the same basic structure shown in Figures 2–7. The G3B3 enthalpies of formation at 0 and 298 K of the larger boron oxides are given in Table 2. The electron affinities (EAs) of B_nO_m at 0 K are given in Table 3. Bond dissociation energies (BDEs) related to the various ways of breaking the bonds in B_nO_m are summarized in Table 4. Geometry parameters and harmonic vibrational frequencies related to the BBO groups in different species are given in Table 5. The vertical detachment energies (VDE) are tabulated in Table

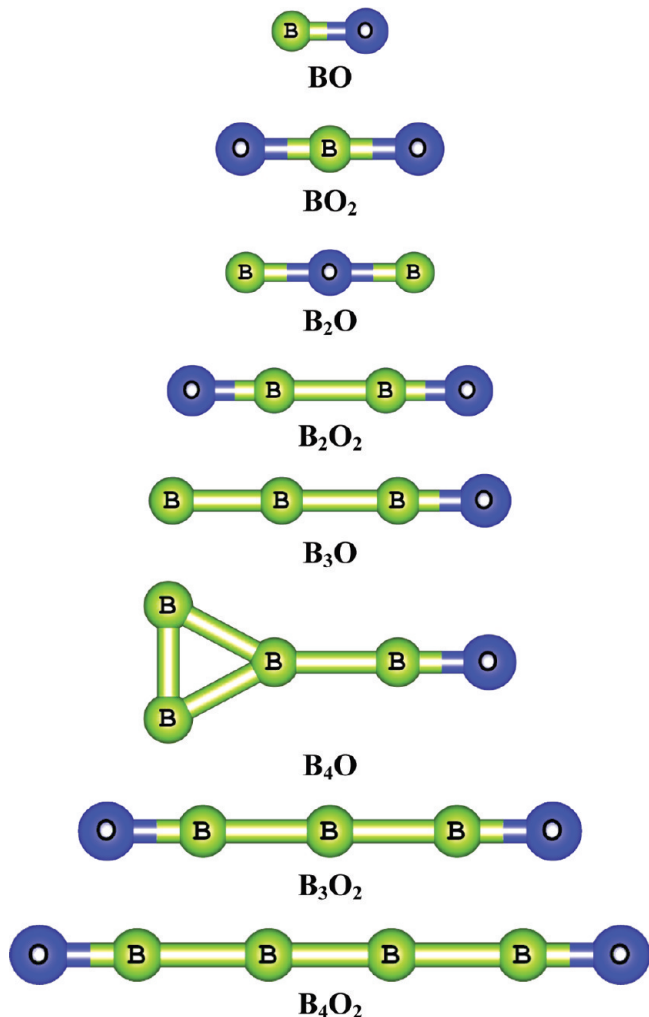


Figure 1. Shapes of the lowest-lying isomers of the neutral B_nO_m clusters with $n = 1–4$ and $m = 1–2$, from ref 23.

6. The total electronic energies and total atomization energies (TAEs), including those of the bare boron clusters (B_n), determined at the same G3B3 method and used for calculating the energies of fragmentation reactions, are listed in the Supporting Information.

Thermochemical Parameters and Structural Stability

B_nO and B_nO_2 with $n = 1–4$ and Their Anions. The series of small boron oxides and dioxides containing up to four boron atoms was extensively examined in our recent study.²³ We calculated these quantities at the G3B3 level for the global minima in Figure 1, in order to benchmark the G3B3 method for these types of compounds. Table 1 shows that the G3B3 heats of formation for the lowest-lying isomers are in very good agreement with the CBS values. The deviation of the G3B3 heats of formation amounts to at most 2 kcal/mol, with an average deviation of ± 1.5 kcal/mol. Except for B_4O , the differences between the EAs predicted at the G3B3 and CCSD(T)/CBS levels are much smaller, ranging from 0.01 eV (for BO_2) to 0.03 eV (for B_2O and B_4O_2); for B_4O , the G3B3 EA differs by 0.15 eV from the CCSD(T)/CBS value. The calculated values are in good agreement with the available experimental results, for example, $EA_{G3B3}(B_4O_2) = 3.17$ eV, $EA_{CCSD(T)/CBS}(B_4O_2) = 3.14$ eV, and $EA_{exp}(B_4O_2) = 3.16 \pm 0.01$ eV, the latter from a photoelectron spectroscopy study of the anion.⁶

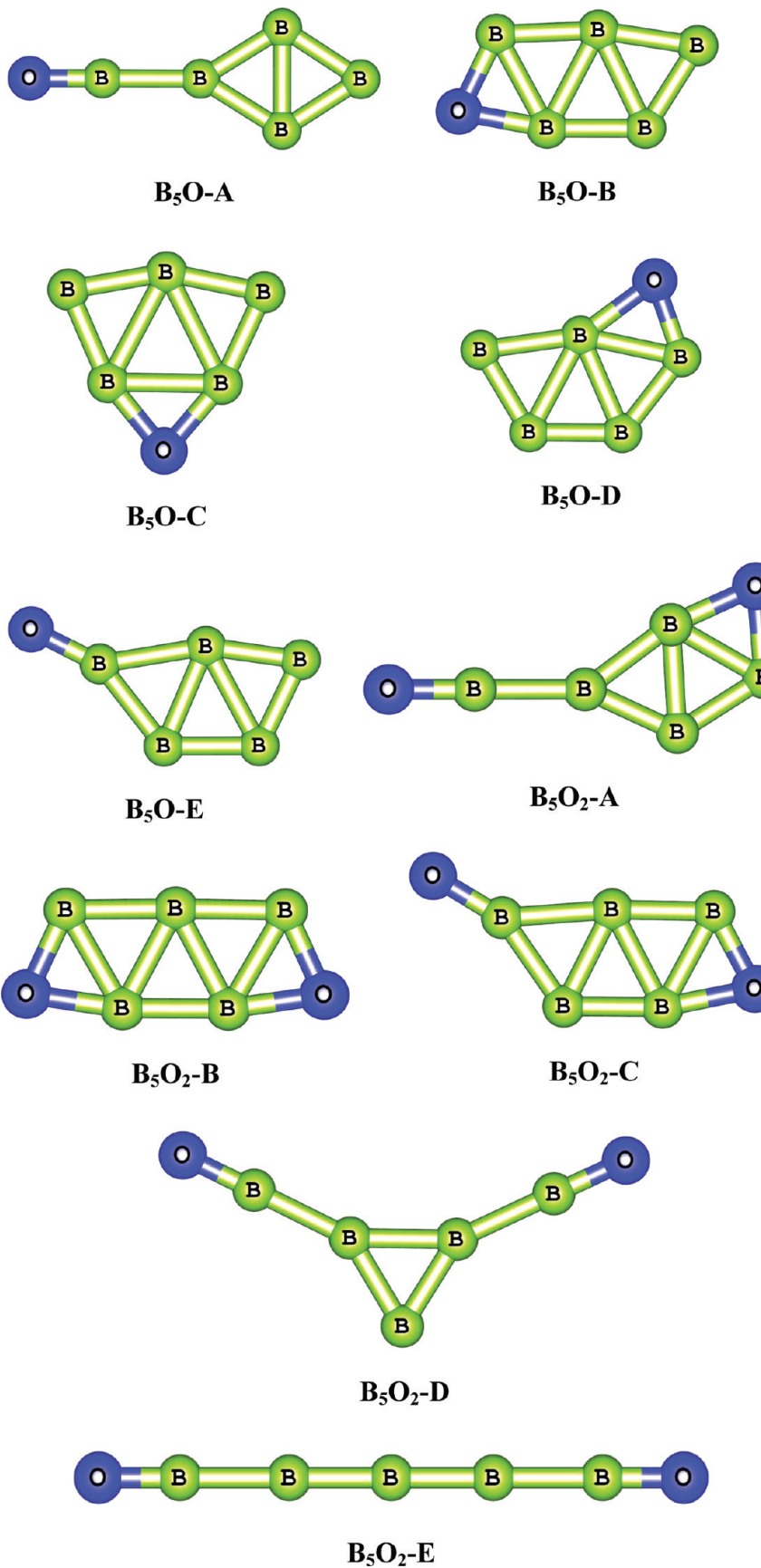


Figure 2. Shapes of the lowest-lying isomers of B_5O and B_5O_2 .

The symmetric neutral BOB (${}^1\Sigma_g^+$) structure is calculated at the G3B3 level to be 15.6 kcal/mol more stable than BBO (${}^1\Sigma^+$). We previously considered²³ only the BOB⁻ isomer. The anion

BBO^- (${}^2\Pi$) is 15.1 kcal/mol lower in energy at the CCSD(T)/CBS level than the more symmetrical isomer BOB⁻ (${}^2\Sigma_g^+$). The quartet–doublet energy separation in BBO⁻ is 3.4 kcal/mol in

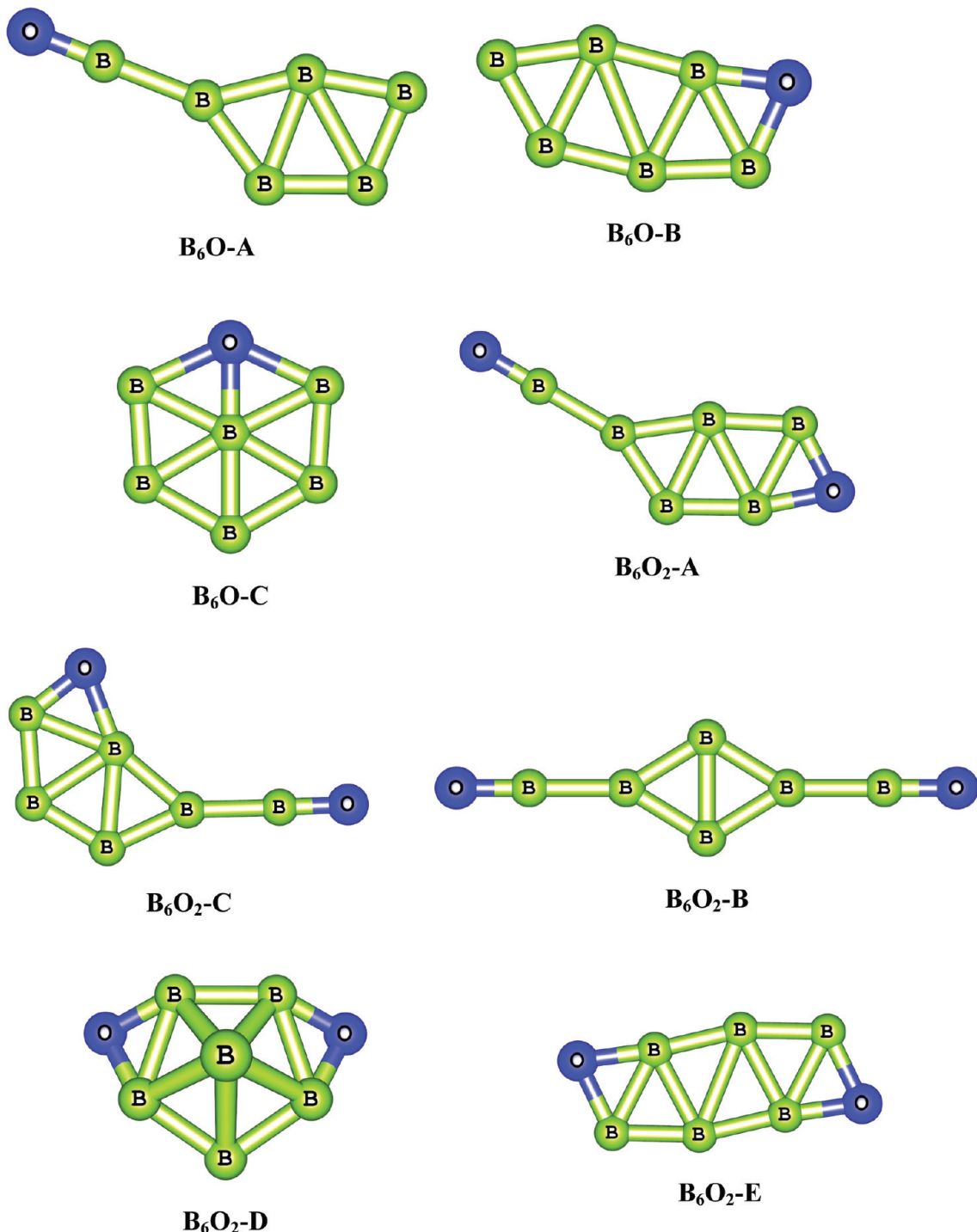


Figure 3. Shapes of the lowest-lying isomers of B_6O and B_6O_2 .

favor of the low spin state. A stabilization of ~ 32 kcal/mol by a single electron attachment for BBO is quite remarkable (Table 1), and is due to a much stronger electron delocalization in the BBO framework. EA(BOB) is only 0.07 eV, and EA(BBO) = 1.44 eV at the CCSD(T)/CBS level is significantly larger (Table 3). As shown in the following sections, formation of stabilized BBO moieties upon electron addition emerges as a consistent and determining feature of the larger boron oxide anions, often leading to reversals in the energy of the different isomers as compared to the energy ordering in the neutrals.

B₅O, B₅O₂, and Anions. The pentaboron monoxide system summarized in Figure 2 includes the following planar structures: B₅O-A (C_{2v}), in which a BO unit binds to one B atom of the B₄

ring along the longer diagonal BB C_2 axis; B₅O-B, with the O bonded to two B atoms of the B₅ ring; two other structures, B₅O-C and B₅O-D, which involve an O-addition to a BB edge of the B₅ ring; and B₅O-E, where the O simply binds to one B atom of the stable B₅ cycle (equivalent to attachment of a BO unit to a BB edge of a B₄ ring). Structure B₅O-B is formed by the substitution of an external B atom from an energetically higher-lying B₆ ring by O. There is no direct O-substitution from the lowest-lying B₆ isomer (C_{5v}) to form B₅O.

Structures B₅O-A and B₅O-B were previously reported²⁴ to be the lowest-lying doublet state of the neutrals B₅O, with a small preference by ~ 3 kcal/mol for B₅O-B. Structures B₅O-B and B₅O-E were also studied previously²⁵ with a large preference

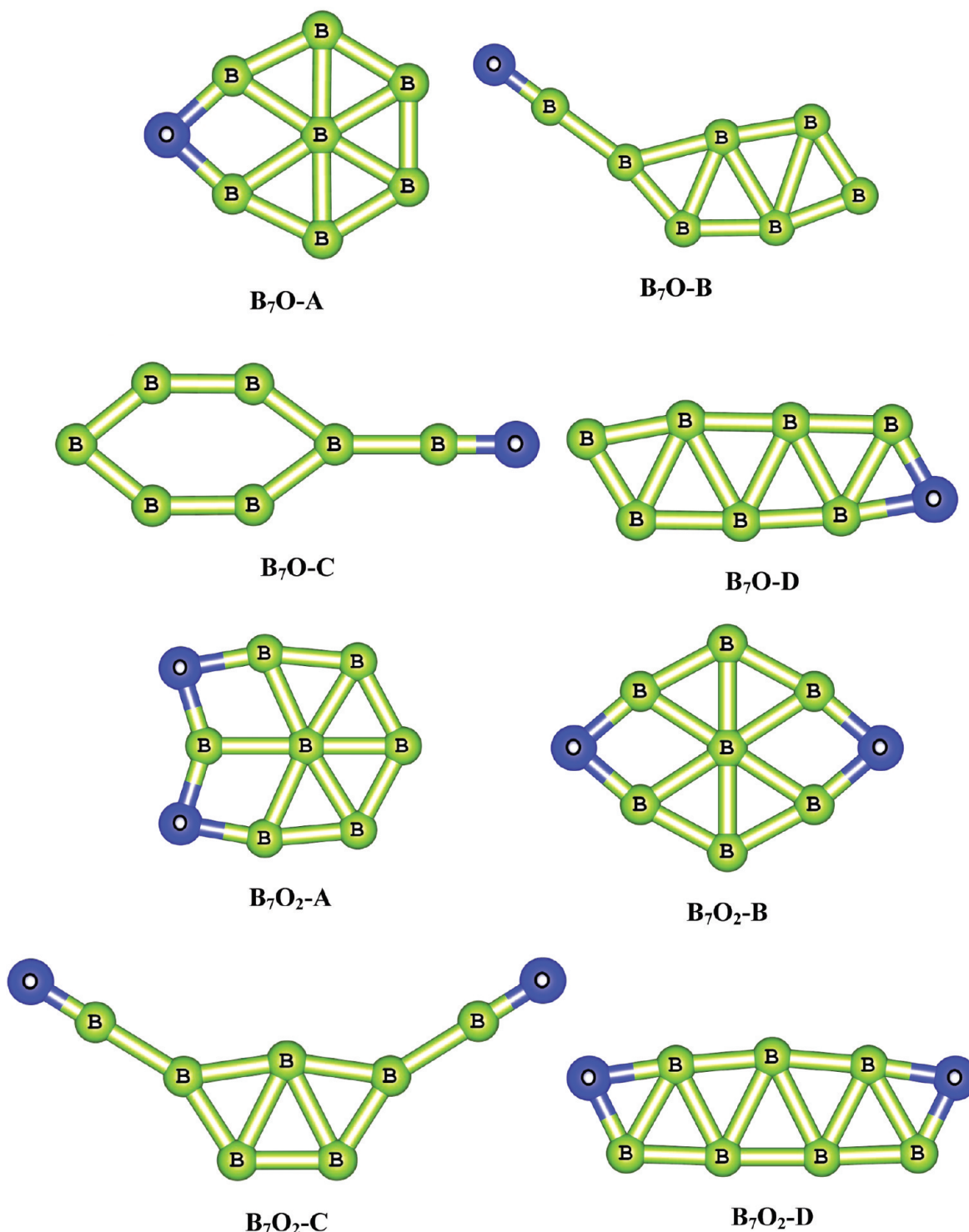


Figure 4. Shapes of the lowest-lying isomers of B_7O and B_7O_2 .

for B_5O -B. The latter authors²⁵ did not investigate the B_5O -A structure. We considered all five structures in both doublet and quartet states for the neutrals. At the G3B3 level, B_5O -B (C_s , $^2A'$) is predicted to be the lowest-energy isomer with B_5O -A (C_{2v} , 2A_1) only 2.1 kcal/mol higher in energy. The high spin structures lie consistently higher in energy. The quartet–doublet energy gap is 21.8 kcal/mol for B_5O -A and 64.0 kcal/mol for B_5O -B.

In our previous study,²³ we suggested that the growth mechanism of small boron oxides is determined by three main factors: (i) formation of BO bonds, (ii) formation or retention of a cyclic B_n unit, and (iii) where possible, combining a stable

boron cycle with the BO bonds. In this model, structure B_5O -A is generated by the interaction of a B_4 ring and a BO bond yielding a single BB bond, and a short terminal BO bond with $r(B-O) = 1.211 \text{ \AA}$ and a vibrational frequency of 2011 cm^{-1} . This BO bond distance is comparable to that in the diatomic with $r(B-O) = 1.209 \text{ \AA}$ and a vibrational frequency of 1953 cm^{-1} . B_5O -B can be generated from addition of O to B_5 or to a $B_4 + BO$ [2 + 2] cycloaddition. Thus, the higher stability of B_5O -A and B_5O -B can be accounted for by the presence of B_4 and B_5 rings, respectively. The fragmentation energies of B_5O -A and B_5O -B to form $B_4 + BO$ are 86.5 and 88.6 kcal/mol, respectively. The B–O binding energies of an O atom to B_5 in

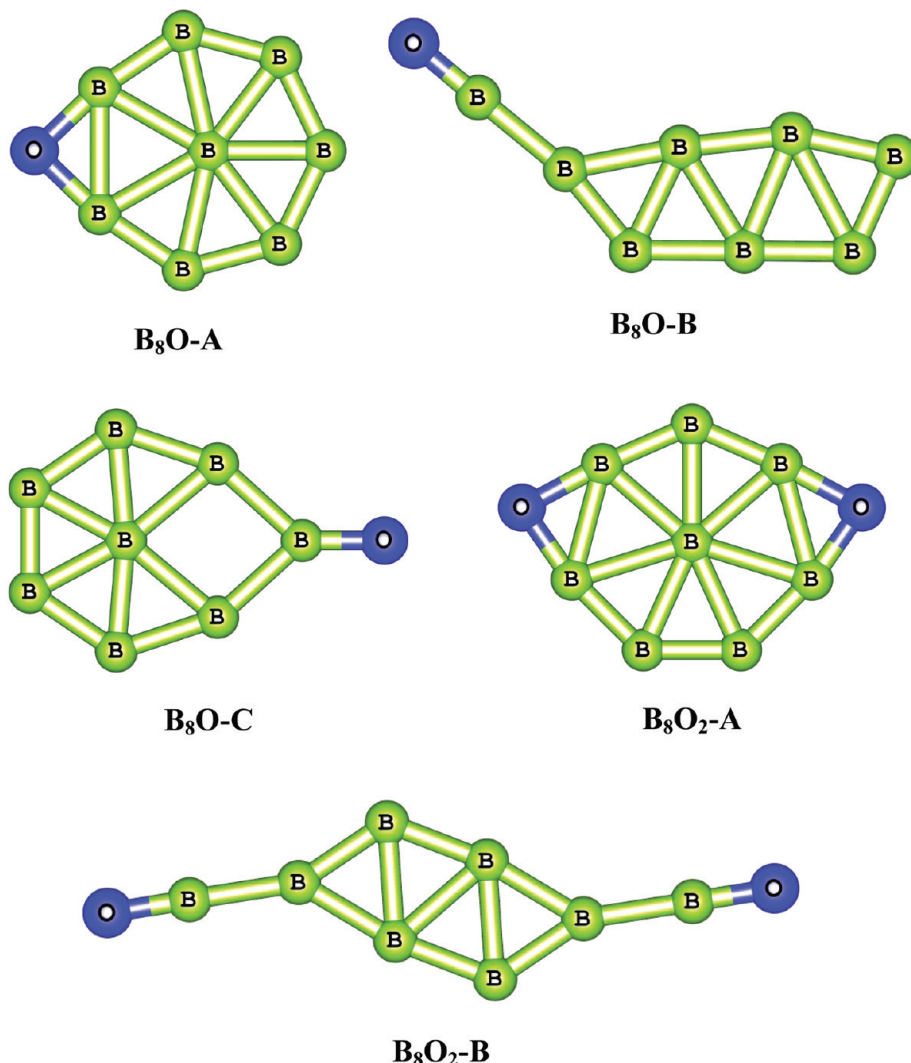


Figure 5. Shapes of the lowest-lying isomers of B₈O and B₈O₂.

B₅O-A and B₅O-B are 171.5 and 173.6 kcal/mol, respectively. Thus it is much easier to break B₅O into B₄ + BO than into B₅ + O, due to the thermodynamic stability of the BO radical.

The same structures were studied for the anionic clusters of B₅O⁻ (Figure 2) for both the singlet and triplet states. Singlet B₅O-A⁻ (C_{2v} , 1A_1) is predicted to be the lowest-lying structure, consistent with the preference for forming an exocyclic BO bond. Triplet B₅O-A (C_{2v} , 3B_2) is the lowest-lying high spin state, with a singlet-triplet separation gap of 17.1 kcal/mol. The singlet state remains lower for B₅O-B⁻ with a singlet-triplet gap of 25.9 kcal/mol, and singlet B₅O-B⁻ is ~30 kcal/mol higher in energy than B₅O-A⁻ (C_{2v} , 1A_1), in contrast to what is predicted for the neutral. Thus, B₅O-A (C_{2v} , 3B_2) is lower in energy than singlet B₅O-B⁻. For B₅O-C⁻, the high spin triplet state is 2.2 kcal/mol more stable than the low spin singlet. For both B₅O-D⁻ and B₅O-E⁻, only triplet state minima could be located. B₅O-E⁻ (C_s , $^3A'$) is a lower-lying isomer, ~17 kcal/mol less stable than the global minimum B₅O-A⁻.

The fragmentation energy of the anion B₅O-A⁻ to B₄ + BO⁻ (108.7 kcal/mol) is smaller than that giving B₄⁻ + BO (129.5 kcal/mol), due to the higher EA of BO. The global adiabatic EA (the global electron affinity is defined as the energy difference between the most stable neutral and most stable anion) of 3.44 eV calculated for B₅O from doublet B₅O-B and singlet B₅O-A⁻ is much larger than that of either BO (2.57 eV) or B₄ (1.67 eV).²³

For B₅O₂ clusters, Drummond et al.²⁴ reported two different structures including B₅O₂-A in which one oxygen is attached to two B atoms of the monoxide B₅O-A and B₅O₂-C, where the second O atom binds to either one B of B₅O-B, or with two B atoms of B₅O-E (Figure 2). Feng et al.²⁵ reported that the linear doublet structure B₅O₂-E in which two BO units are bound to a linear B₃ is the most stable. We considered the various B₅O₂ structures shown in Figure 2 that include two new high symmetry structures denoted as B₅O₂-B and B₅O₂-D, which were not discussed previously. Our G3B3 results concur with the result that B₅O₂-A (C_s , $^2A'$) is the most stable neutral form among several low-lying isomers. The second lowest lying isomer B₅O₂-D (C_{2v} , 2B_2), constructed from two BO units plus the triangular B₃ cycle, is only 4.3 kcal/mol higher in energy. Linear B₅O₂-E ($^2\Sigma_g^+$) is only 4.5 kcal/mol less stable than B₅O₂-A. The alternative B₅O₂-B (C_{2v} , 2B_2) formed by attachment of two oxygens at two opposite sides of B₅ is 6.9 kcal/mol higher in energy than B₅O₂-A. Thus there are four isomers all within 7 kcal/mol. The terminal BO bond of B₅O₂-A has a short B-O bond distance and a stretching frequency, very similar to these values for the monoxide B₅O-A.

The reaction to remove an O atom, B₅O₂-A → B₅O-A + O(³P), is endothermic by 172.3 kcal/mol. Loss of both O atoms from B₅O₂-B to generate cyclic B₅ (C_{2v} , 2B_2) requires 342.3 kcal/mol.

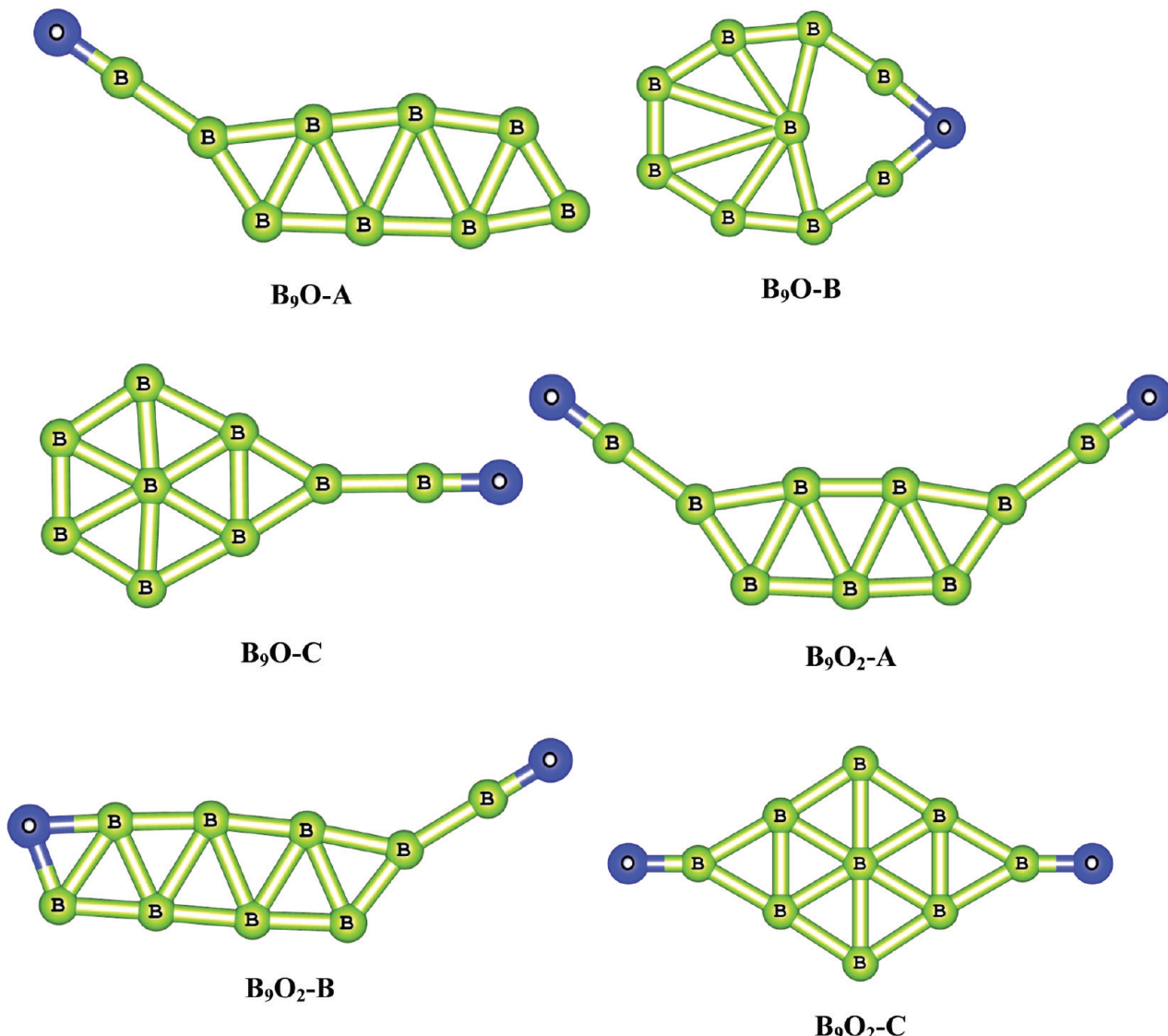


Figure 6. Shapes of the lowest-lying isomers of B_9O and B_9O_2 .

The ELF plots of the neutral B_5O_2 -A show that the total electron populations of basins enclosing two B and O atoms is ~ 3.0 e, which is much smaller than that of the nonbonding O(BO) basin (4.5 e). The V(B-O) basin contains 3.6 e consistent with an increase in the BO bond strength.

Attachment of one electron to B_5O_2 leads to structure $B_5O_2^-$ (C_{2v} , 1A_1) becoming the most stable $B_5O_2^-$ anion isomer. The next higher energy isomer is linear $B_5O_2^-E^-$, 15.4 kcal/mol higher in energy. Other isomers are less stable and are >20 kcal/mol higher in energy than $B_5O_2^-D^-$. Binding of two BO units to the B_3^- cycle to form $B_5O_2^-D^-$ is exothermic by -218.0 kcal/mol, and binding a BO^- anion to the most stable structure for B_4O again forming $B_5O_2^-D^-$ is exothermic by -225.9 kcal/mol. The higher stability of $B_5O_2^-D^-$ provides another demonstration of the preferred combination of BO bonds with a boron cycle. The global adiabatic EA(B_5O_2) = 4.34 eV is even larger than that for B_5O .

B_6O , B_6O_2 , and Their Anions. Among various arrangements of B_6O , B_6O -A (C_s , $^1A'$) (Figure 3) is the most stable structure for closed-shell neutral B_6O . It can be generated by condensation of BO with the most stable form of the five-membered ring B_5 . The second lowest lying isomer is B_6O -B ($^1A'$), at 21.6 kcal/mol higher in energy. In B_6O -B, the BO unit is bonded to a BB edge of B_5 through a [2 + 2] cycloaddition with the formation

of an additional B-B bond. The other B_6O isomers including B_6O -C are located at >30 kcal/mol higher in energy than B_6O -A. These results agree well with the molecular dynamics (MD) predictions by Drummond et al.²⁴ but are not in agreement with Feng et al.,²⁵ who predicted that B_6O -B ($^1A'$) is the lowest-lying isomer.

Condensation of a BO radical with the five-membered B_5 ring to generate B_6O -A ($^1A'$) is exothermic by -112.0 kcal/mol, much larger than the similar reaction of $BO + cyclo-B_4$ leading to B_6O -A (-86.5 kcal/mol, cf. Table 4). In B_6O -A, the bond distance and stretching frequency of the terminal BO are nearly identical to those of B_5O -A and B_5O_2 -A and are close to the values for the diatomic radical BO. The ELF plots of B_6O -A indicate a basin V(BO) of 3.7 e and two basins V(BBB) containing 3.3 and 2.8 e. A strong electron delocalization is present, and the multicenter bonds enhance the stability of B_6O -A.

Addition of one electron to the LUMO of B_6O -A does not lead to much geometry distortion, and the resulting anion B_6O^- (C_s , $^2A''$) is predicted to be the most stable B_6O^- cluster. The terminal BO bond distance is slightly stretched in comparison with the neutral distance in B_6O -A. The global adiabatic EA(B_6O) = 2.69 eV is quite large considering the closed-shell configuration of the neutral. Condensation of BO^- to B_5 to

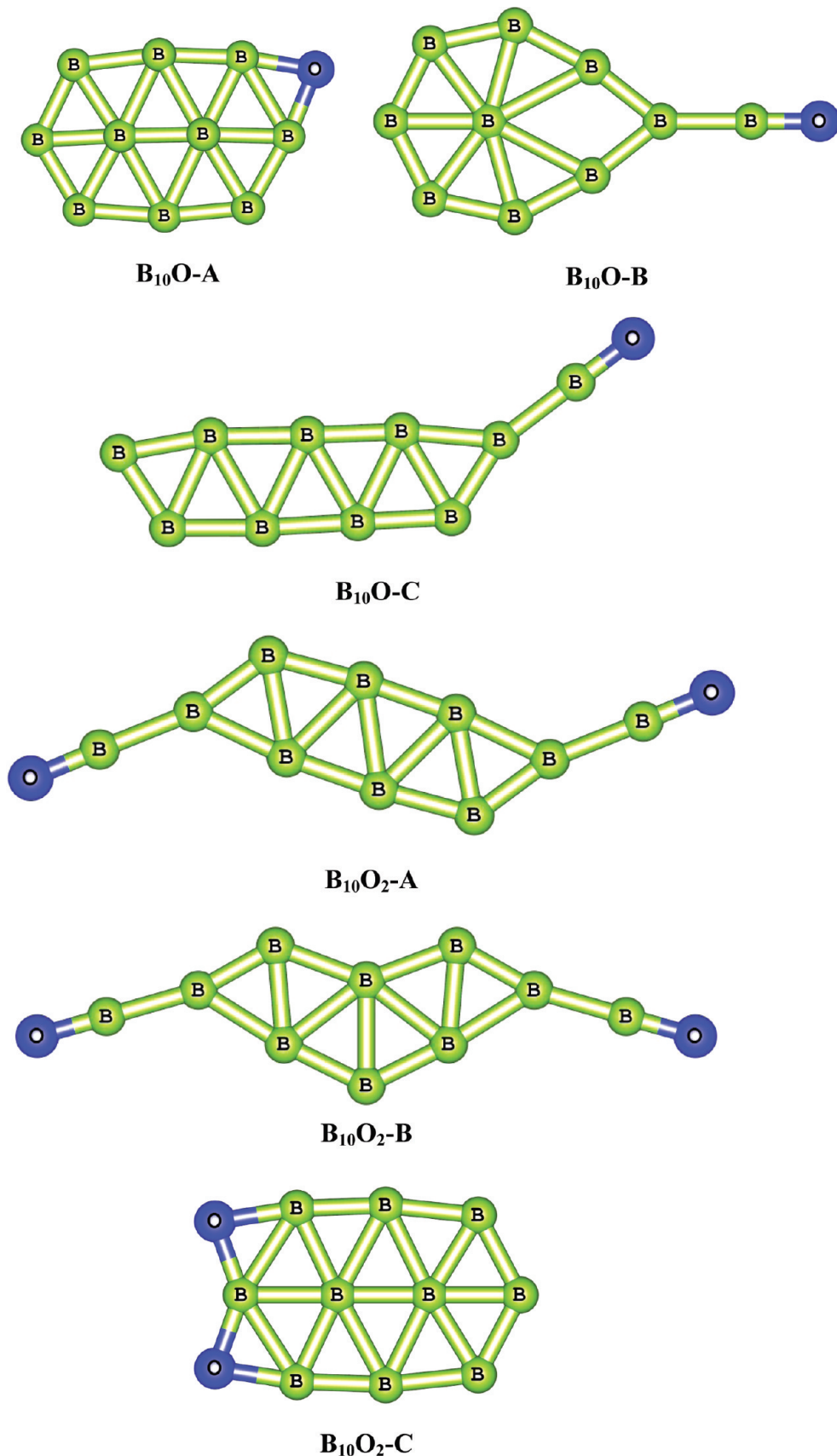


Figure 7. Shapes of the lowest-lying isomers of $\mathbf{B}_{10}\mathbf{O}$ and $\mathbf{B}_{10}\mathbf{O}_2$.

generate $\mathbf{B}_6\mathbf{O}\text{-A}^-$ is exothermic by -114.7 kcal/mol, ~ 3 kcal/mol larger than the corresponding condensation energy for the neutral $\mathbf{B}_6\mathbf{O}\text{-A}$ (Table 4).

The structural features of hexaboron dioxide are also summarized in Figure 3. $\mathbf{B}_6\mathbf{O}_2\text{-A}$ with the second O atom bonding with a BB edge of $\mathbf{B}_6\mathbf{O}\text{-A}$ was reported to be the global

TABLE 2: G3B3 Calculated Heats of Formation (ΔH_f , kcal/mol) for the Boron Oxides B_nO_m ($n = 5-10$, $m = 1-2$)

structure	label ^a	symmetry, state	$\Delta H_f(0\text{ K})$	$\Delta H_f(298\text{ K})$
B_5O	$B_5O\text{-A}$	$C_{2v}, ^2A_1$	142.4	144.1
	$B_5O\text{-A}$	$C_{2v}, ^4B_2$	164.2	166.3
	$B_5O\text{-B}$	$C_s, ^2A'$	140.3	141.4
	$B_5O\text{-B}$	$C_s, ^4A''$	204.3	205.6
	$B_5O\text{-C}$	$C_{2v}, ^2B_2$	160.5	161.5
	$B_5O\text{-C}$	$C_{2v}, ^4A_1$	187.7	189.1
	$B_5O\text{-D}$	$C_s, ^2A'$	149.5	150.7
	$B_5O\text{-D}$	$C_s, ^4A''$	193.6	194.6
	$B_5O\text{-E}$	$C_s, ^2A'$	157.8	159.4
	$B_5O\text{-E}$	$C_s, ^4A'$	181.7	183.5
B_5O^-	$B_5O\text{-A}^-$	$C_{2v}, ^1A_1$	60.9	62.6
	$B_5O\text{-A}^-$	$C_{2v}, ^3A_1$	78.0	79.8
	$B_5O\text{-B}^-$	$C_s, ^1A'$	90.3	91.4
	$B_5O\text{-B}^-$	$C_s, ^3A''$	116.2	117.3
	$B_5O\text{-C}^-$	$C_{2v}, ^1A_1$	109.1	110.0
	$B_5O\text{-C}^-$	$C_{2v}, ^3B_1$	106.9	108.2
	$B_5O\text{-D}^-$	$C_s, ^3A''$	108.2	109.2
	$B_5O\text{-E}^-$	$C_s, ^3A'$	78.0	79.8
B_5O_2	$B_5O_2\text{-A}$	$C_s, ^2A'$	29.1	30.2
	$B_5O_2\text{-B}$	$C_{2v}, ^2B_2$	36.0	36.6
	$B_5O_2\text{-C}$	$C_s, ^2A'$	43.6	44.5
	$B_5O_2\text{-D}$	$C_{2v}, ^2B_2$	33.4	34.8
	$B_5O_2\text{-E}$	$D_{\infty h}, ^2\Pi_u$	33.6	35.4
$B_5O_2^-$	$B_5O_2\text{-A}^-$	$C_s, ^1A'$	-50.2	-49.2
	$B_5O_2\text{-A}^-$	$C_s, ^3A'$	-0.2	0.8
	$B_5O_2\text{-B}^-$	$C_{2v}, ^1A_1$	-13.1	-12.4
	$B_5O_2\text{-D}^-$	$C_{2v}, ^1A_1$	-70.9	-69.5
	$B_5O_2\text{-D}^-$	$C_{2v}, ^3A_1$	-44.8	-43.1
	$B_5O_2\text{-E}^-$	$D_{\infty h}, ^1\Sigma^+$	-55.5	-53.7
B_6O	$B_6O\text{-A}$	$C_s, ^1A'$	145.1	147.1
	$B_6O\text{-B}$	$C_s, ^1A'$	166.7	168.3
	$B_6O\text{-C}$	$C_{2v}, ^1A_1$	234.2	235.1
B_6O^-	$B_6O\text{-A}^-$	$C_s, ^2A''$	83.1	84.7
	$B_6O\text{-B}^-$	$C_s, ^2A''$	120.2	121.9
	$B_6O\text{-C}^-$	$C_{2v}, ^2A_1$	174.6	175.9
B_6O_2	$B_6O_2\text{-A}$	$C_s, ^1A'$	25.3	26.5
	$B_6O_2\text{-B}$	$D_{2h}, ^1A_g$	32.0	33.8
	$B_6O_2\text{-C}$	$C_s, ^1A'$	35.5	36.7
	$B_6O_2\text{-D}$	$C_s, ^1A'$	80.3	80.7
	$B_6O_2\text{-E}$	$C_{2h}, ^1A_g$	47.7	48.5
$B_6O_2^-$	$B_6O_2\text{-A}^-$	$C_s, ^2A'$	-7.2	-6.1
	$B_6O_2\text{-B}^-$	$D_{2h}, ^2A_g$	-51.0	-49.3
	$B_6O_2\text{-C}^-$	$C_s, ^2A'$	-20.8	-19.4
	$B_6O_2\text{-E}^-$	$C_{2h}, ^2B_g$	7.6	8.6
B_7O	$B_7O\text{-A}$	$C_{2v}, ^2A_2$	170.9	171.7
	$B_7O\text{-B}$	$C_s, ^2A''$	180.7	183.0
	$B_7O\text{-C}$	$C_{2v}, ^2B_1$	190.2	191.8
	$B_7O\text{-D}$	$C_s, ^2A'$	209.8	211.0
B_7O^-	$B_7O\text{-A}^-$	$C_{2v}, ^1A_1$	102.9	104.0
	$B_7O\text{-B}^-$	$C_s, ^1A'$	101.6	103.4
B_7O_2	$B_7O_2\text{-C}^-$	$C_{2v}, ^1A_1$	110.9	112.4
	$B_7O_2\text{-A}$	$C_{2v}, ^2A_2$	57.6	57.8
	$B_7O_2\text{-B}$	$D_{2h}, ^2B_{1g}$	59.8	59.9
$B_7O_2^-$	$B_7O_2\text{-C}$	$C_{2v}, ^2B_1$	59.8	62.0
	$B_7O_2\text{-D}$	$C_{2v}, ^2A_1$	86.4	87.6
	$B_7O_2\text{-A}^-$	$C_{2v}, ^1A_1$	4.5	5.1
	$B_7O_2\text{-B}^-$	$D_{2h}, ^1A_g$	-11.2	-10.7
B_8O	$B_8O\text{-C}^-$	$C_{2v}, ^1A_1$	-25.9	-24.3
	$B_8O\text{-D}^-$	$C_{2v}, ^1A_1$	34.2	35.0
	$B_8O\text{-A}$	$C_{2v}, ^1A_1$	168.2	169.9
B_8O^-	$B_8O\text{-B}$	$C_s, ^1A'$	198.2	200.7
	$B_8O\text{-C}$	$C_{2v}, ^1A_1$	253.5	254.9
	$B_8O\text{-A}^-$	$C_{2v}, ^2B_1$	113.1	114.7
B_8O_2	$B_8O\text{-B}^-$	$C_s, ^2A'$	109.2	111.4
	$B_8O\text{-C}^-$	$C_{2v}, ^2A_2$	160.6	162.2
	$B_8O_2\text{-A}$	$C_{2v}, ^1A_1$	56.2	57.5
$B_8O_2^-$	$B_8O_2\text{-B}$	$C_{2h}, ^1A_g$	77.7	80.1
	$B_8O_2\text{-A}^-$	$C_{2v}, ^2A_2$	15.3	16.8
B_9O	$B_8O_2\text{-B}^-$	$C_{2h}, ^2B_g$	-17.4	-15.3
	$B_9O\text{-A}$	$C_s, ^2A'$	214.7	217.2
	$B_9O\text{-B}$	$C_{2v}, ^2B_1$	222.2	224.8

TABLE 2: Continued

structure	label ^a	symmetry, state	$\Delta H_f(0 \text{ K})$	$\Delta H_f(298 \text{ K})$
B_9O^-	$\text{B}_9\text{O-C}$	$C_{2v}, ^2\text{B}_2$	228.0	230.2
	$\text{B}_9\text{O-A}^-$	$C_s, ^1\text{A}'$	129.3	131.9
	$\text{B}_9\text{O-B}^-$	$C_{2v}, ^1\text{A}_1$	154.4	157.0
	$\text{B}_9\text{O-C}^-$	$C_{2v}, ^1\text{A}_1$	132.0	133.9
B_{9O_2}	$\text{B}_{9\text{O}_2}\text{-A}$	$C_{2v}, ^2\text{A}_2$	94.5	97.0
	$\text{B}_{9\text{O}_2}\text{-B}$	$C_s, ^2\text{A}'$	104.4	106.3
	$\text{B}_{9\text{O}_2}\text{-C}$	$D_{2h}, ^2\text{B}_{1g}$	154.5	156.2
B_{9O_2}^-	$\text{B}_{9\text{O}_2}\text{-A}^-$	$C_{2v}, ^1\text{A}_1$	-13.6	-11.4
	$\text{B}_{9\text{O}_2}\text{-C}^-$	$D_{2h}, ^1\text{A}_g$	85.7	87.6
$\text{B}_{10\text{O}}$	$\text{B}_{10\text{O}}\text{-A}$	$C_s, ^1\text{A}'$	210.9	212.5
	$\text{B}_{10\text{O}}\text{-B}$	$C_{2v}, ^1\text{A}_1$	232.2	234.3
	$\text{B}_{10\text{O}}\text{-C}$	$C_s, ^1\text{A}'$	234.4	237.3
$\text{B}_{10\text{O}}^-$	$\text{B}_{10\text{O}}\text{-A}^-$	$C_s, ^2\text{A}'$	149.5	151.4
	$\text{B}_{10\text{O}}\text{-B}^-$	$C_{2v}, ^2\text{A}_2$	133.5	136.3
	$\text{B}_{10\text{O}}\text{-C}^-$	$C_s, ^2\text{A}''$	162.0	164.7
B_{10O_2}	$\text{B}_{10\text{O}_2}\text{-A}$	$C_{2h}, ^1\text{A}_g$	102.4	105.0
	$\text{B}_{10\text{O}_2}\text{-B}$	$C_{2v}, ^1\text{A}_1$	111.3	114.0
	$\text{B}_{10\text{O}_2}\text{-C}$	$C_{2v}, ^1\text{A}_1$	106.2	107.3
$\text{B}_{10\text{O}_2}^-$	$\text{B}_{10\text{O}_2}\text{-A}^-$	$C_{2h}, ^2\text{B}_u$	20.7	23.3
	$\text{B}_{10\text{O}_2}\text{-B}^-$	$C_{2v}, ^2\text{A}_1$	34.9	37.5
	$\text{B}_{10\text{O}_2}\text{-C}^-$	$C_{2v}, ^2\text{B}_2$	51.3	52.8

^a See definitions of the structures in Figures 2–7.

TABLE 3: Adiabatic Electronic Affinities (EA, eV) at 0 K of the Boron Oxides B_nO_m for $n = 1\text{--}10$, $m = 1\text{--}2$

neutral	anion	EA		
		G3B3	CBS ^a	exptl ^c
$\text{BO} ({}^2\Sigma^+)$	$\text{BO}^- ({}^1\Sigma^+)$	2.57	2.51	2.508 ± 0.008
$\text{OBO} ({}^2\Pi_g)$	$\text{BO}_2^- ({}^1\Sigma_g^+)$	4.47	4.48	4.51
$\text{BOB} ({}^1\Sigma_g^+)$	$\text{BOB}^- ({}^2\Sigma_g^+)$	0.10	0.07	
$\text{BBO} ({}^1\Sigma_g^+)$	$\text{BBO}^- ({}^2\Pi)$	1.47	1.44 ^b	
$\text{OBBO} ({}^1\Sigma_g^+)$	$\text{OBBO}^- ({}^2\text{B}_u)$	0.37	0.37	
$\text{BBBO} ({}^4\Sigma^-)$	$\text{B}_3\text{O}^- ({}^3\text{A}_1)$	2.05	2.05	
$\text{OB}_3\text{O} ({}^2\Pi_g)$	$\text{B}_3\text{O}_2^- ({}^3\Sigma_u^-)$	2.97	2.94	2.94 ± 0.002
$\text{B}_4\text{O} ({}^1\text{A}_1)$	$\text{B}_4\text{O}^- ({}^2\text{A}_1)$	2.73	2.58	
$\text{B}_4\text{O}_2 ({}^3\Sigma_g^-)$	$\text{B}_4\text{O}_2^- ({}^2\Pi)$	3.17	3.14	3.16 ± 0.01
$\text{B}_5\text{O-B} ({}^2\text{A}')$	$\text{B}_5\text{O-A}^- ({}^1\text{A}_1)$	3.44		
$\text{B}_5\text{O}_2\text{-A} ({}^2\text{A}')$	$\text{B}_5\text{O}_2\text{-D}^- ({}^1\text{A}_1)$	4.34		
$\text{B}_6\text{O-A} ({}^1\text{A}')$	$\text{B}_6\text{O-A}^- ({}^2\text{A}'')$	2.69		
$\text{B}_6\text{O}_2\text{-A} ({}^1\text{A}')$	$\text{B}_6\text{O}_2\text{-B}^- ({}^2\text{A}_g)$	3.31		
$\text{B}_7\text{O-A} ({}^2\text{A}_2)$	$\text{B}_7\text{O-B}^- ({}^1\text{A}')$	3.00		
$\text{B}_7\text{O}_2\text{-A} ({}^2\text{A}_2)$	$\text{B}_7\text{O}_2\text{-B}^- ({}^1\text{A}_1)$	3.62		
$\text{B}_8\text{O-A} ({}^1\text{A}_1)$	$\text{B}_8\text{O-B}^- ({}^2\text{A}')$	2.56		
$\text{B}_8\text{O}_2\text{-A} ({}^1\text{A}_1)$	$\text{B}_8\text{O}_2\text{-C}^- ({}^2\text{B}_g)$	3.19		
$\text{B}_9\text{O-A} ({}^2\text{A}'')$	$\text{B}_9\text{O-A}^- ({}^1\text{A}')$	3.70		
$\text{B}_9\text{O}_2\text{-A} ({}^2\text{A}_2)$	$\text{B}_9\text{O}_2\text{-A}^- ({}^1\text{A}_1)$	4.69		
$\text{B}_{10}\text{O-A} ({}^1\text{A}')$	$\text{B}_{10}\text{O-B}^- ({}^2\text{A}_2)$	3.36		
$\text{B}_{10}\text{O}_2\text{-A} ({}^1\text{A}_g)$	$\text{B}_{10}\text{O}_2\text{-A}^- ({}^2\text{B}_u)$	3.54		

^a Calculated CCSD(T)/CBS values taken from ref 23.

^b CCSD(T)/CBS values, this work. ^c Experimental values taken from ref 6.

equilibrium structure in one study,²⁴ and structure $\text{B}_6\text{O}_2\text{-C}$ was predicted to be the most stable isomer in a second study.²⁵ We considered five different isomers for B_6O_2 (Figure 3). Beside $\text{B}_6\text{O}_2\text{-A}$ and $\text{B}_6\text{O}_2\text{-C}$, we also considered the high symmetry $\text{B}_6\text{O}_2\text{-B}$ isomer with two BO groups and a B_4 ring, the C_{2v} isomer $\text{B}_6\text{O}_2\text{-D}$ with two O atoms bonded with two BB edges of the most stable B_6 (C_{5v}) isomer, and finally planar $\text{B}_6\text{O}_2\text{-E}$, where the second O is bonded to two B atoms on the opposite side of $\text{B}_6\text{O-B}$. Our results concur with the finding²⁴ that $\text{B}_6\text{O}_2\text{-A}$ ($C_s, ^1\text{A}'$) is the global energy minimum, followed by $\text{B}_6\text{O}_2\text{-B}$ ($D_{2h}, ^1\text{A}_g$) 6.7 kcal/mol higher in energy. Singlet $\text{B}_6\text{O}_2\text{-C}$ is a local minimum 10.1 kcal/mol less stable than $\text{B}_6\text{O}_2\text{-A}$. The higher stabilities of $\text{B}_6\text{O}_2\text{-A}$ and $\text{B}_6\text{O}_2\text{-B}$ can be understood from the structures of B_5O discussed above. The presence of a B_5 ring as in structures $\text{B}_5\text{O-B}$ and $\text{B}_6\text{O}_2\text{-A}$ is preferred over the B_4 ring in $\text{B}_5\text{O-A}$ and $\text{B}_6\text{O}_2\text{-B}$.

The reactions that break $\text{B}_6\text{O}_2\text{-A}$ into the fragments $\text{BO} + \text{B}_5\text{O-B}$ or $\text{O} + \text{B}_6\text{O-A}$ are endothermic by 117.2 and 178.8 kcal/mol, respectively. The first value is smaller than the second, due to the stability of the BO and B_5O radicals. Binding of BO to $\text{B}_5\text{O-A}$ to produce $\text{B}_6\text{O}_2\text{-B}$ is exothermic by -112.6 kcal/mol. The terminal BO bond distances and vibrational frequencies of $\text{B}_6\text{O}_2\text{-A}$ and $\text{B}_6\text{O}_2\text{-B}$ are comparable to each other and to other terminal BO bonds.

The high symmetry $\text{B}_6\text{O}_2\text{-B}^- (D_{2h}, ^2\text{A}_g)$ anion becomes the lowest-lying isomer and is 43.9 kcal/mol below $\text{B}_6\text{O}_2\text{-A}^-$. The terminal BO bond distance of $\text{B}_6\text{O}_2\text{-A}^-$ elongates slightly in comparison to $\text{B}_6\text{O}_2\text{-A}$, and the BB distance remains almost unchanged on electron attachment, slightly decreasing from 1.636 to 1.633 Å. The reactions for binding of either BO to singlet $\text{B}_5\text{O-A}^-$ or BO^- to doublet $\text{B}_5\text{O-A}$, both generating the anion $\text{B}_6\text{O}_2\text{-B}^-$, are exothermic by -114.3 and -136.4 kcal/mol, respectively. As found for BBO , the addition of an electron stabilized the linear BBO units in $\text{B}_6\text{O}_2\text{-B}^-$ and enhances its stability relative to $\text{B}_6\text{O}_2\text{-A}^-$. The predicted global adiabatic EA for closed-shell B_6O_2 of 3.31 eV is even larger than that for B_6O .

B₇O, B₇O₂, and Their Anions. The four different B₇O structures shown in Figure 4 correspond to the lowest-lying isomers on the doublet potential energy surface. The high symmetry structure $\text{B}_7\text{O-A} (C_{2v}, ^2\text{A}_2)$ is predicted to be the most stable isomer, lying 9.7 kcal/mol below structure $\text{B}_7\text{O-B} (C_s, ^2\text{A}'')$, consistent with previous work.²⁴ The preference of $\text{B}_7\text{O-A}$ over other isomers is due to the addition of O to the most stable B₇ unit (D_{6h}). $\text{B}_7\text{O-B}$ arises from a $\text{BO} + \text{B}_6$ recombination, but the B_6 unit does not correspond to the most stable form. However, condensation of BO with the lowest-lying isomer of B_6 , which is a pentagon (C_{5v}), does not lead to a low-energy B_7O isomer either. The decomposition reactions $\text{B}_7\text{O-A} \rightarrow \text{O} + \text{B}_7$ and $\text{B}_7\text{O-B} \rightarrow \text{BO} + \text{B}_6$ are endothermic by 174.6 and 111.6 kcal/mol, respectively (Table 4).

Structure $\text{B}_7\text{O-B}^- (C_s, ^1\text{A}')$ becomes slightly more stable than $\text{B}_7\text{O-A}^- (C_{2v}, ^1\text{A}_1)$, but the small energy difference of only 1.3 kcal/mol suggests they are quasi-degenerate. The triplet state of $\text{B}_7\text{O-B}^- (C_s, ^3\text{A}'')$ is also a low-energy species, with a triplet-singlet gap of 3.1 kcal/mol. The condensation of $\text{BBO}^- + \text{B}_5$ producing $\text{B}_7\text{O-B}^- ({}^1\text{A}')$ is exothermic by -175.8 kcal/mol.

TABLE 4: Energies (ΔH_r in kcal/mol) of the Decomposition Reactions of the Boron Oxides

decomposition reaction	$\Delta H_r(0\text{ K})$	$\Delta H_r(298\text{ K})$
$B_5O\text{-A}({}^2A_1) \rightarrow B_4({}^1A_g) + BO({}^2\Sigma^+)$	86.5	87.3
$B_5O\text{-A}({}^2A_1) \rightarrow B_5({}^2B_2) + O({}^3P)$	171.5	172.7
$B_5O\text{-B}({}^2A') \rightarrow B_4({}^1A_g) + BO({}^2\Sigma^+)$	88.6	90.0
$B_5O\text{-B}({}^2A') \rightarrow B_5({}^2B_2) + O({}^3P)$	173.6	175.4
$B_5O\text{-A}^-({}^1A_1) \rightarrow B_4({}^1A_g) + BO^-({}^1\Sigma^+)$	108.7	109.5
$B_5O\text{-A}^-({}^1A_1) \rightarrow B_4^-({}^2B_{1u}) + BO({}^2\Sigma^+)$	129.5	130.1
$B_5O_2\text{-A}({}^2A') \rightarrow B_5O\text{-A}({}^2A_1) + O({}^3P)$	172.3	173.9
$B_5O_2\text{-D}^-({}^1A_1) \rightarrow B_3({}^2A'_1) + BO({}^2\Sigma^+) + BO^-({}^1\Sigma^+)$	225.9	227.5
$B_5O_2\text{-D}^-({}^1A_1) \rightarrow B_3^-({}^2A'_1) + 2BO({}^2\Sigma^+)$	218.0	219.6
$B_6O\text{-A}({}^1A') \rightarrow B_5({}^2B_2) + BO({}^2\Sigma^+)$	112.0	112.6
$B_6O\text{-A}^-({}^2A'') \rightarrow B_5({}^2B_2) + BO^-({}^1\Sigma^+)$	114.7	115.7
$B_6O\text{-A}^-({}^2A'') \rightarrow B_5^-({}^1A_1) + BO({}^2\Sigma^+)$	116.9	117.8
$B_6O_2\text{-A}({}^1A') \rightarrow B_6O\text{-A}({}^1A') + O({}^3P)$	178.8	180.6
$B_6O_2\text{-A}({}^1A') \rightarrow B_5O\text{-B}({}^2A') + BO({}^2\Sigma^+)$	117.2	117.8
$B_6O_2\text{-B}^-({}^2A_g) \rightarrow B_4({}^1A_g) + BO({}^2\Sigma^+) + BO^-({}^1\Sigma^+)$	222.8	224.3
$B_6O_2\text{-B}^-({}^2A_g) \rightarrow B_4^-({}^2B_{1u}) + 2BO({}^2\Sigma^+)$	243.6	244.9
$B_7O\text{-A}({}^2A_2) \rightarrow B_7({}^2B_2) + O({}^3P)$	174.6	176.6
$B_7O\text{-A}({}^2A_2) \rightarrow B_6({}^1A_1) + BO({}^2\Sigma^+)$	116.5	118.1
$B_7O\text{-B}^-({}^1A') \rightarrow B_6({}^1A_1) + BO^-({}^1\Sigma^+)$	126.5	127.1
$B_7O\text{-B}^-({}^1A') \rightarrow B_6^-({}^2B_{2g}) + BO({}^2\Sigma^+)$	111.4	112.5
$B_7O_2\text{-A}({}^2A_2) \rightarrow B_7O\text{-A}({}^2A_2) + O({}^3P)$	172.3	173.9
$B_7O_2\text{-B}^-({}^1A_1) \rightarrow B_5({}^2B_2) + BO^-({}^1\Sigma^+) + BO({}^2\Sigma^+)$	225.9	227.6
$B_7O_2\text{-B}^-({}^1A_1) \rightarrow B_5^-({}^1A_1) + 2BO({}^2\Sigma^+)$	228.1	229.7
$B_7O_2\text{-B}^-({}^1A_1) \rightarrow B_6O\text{-A}({}^1A') + BO^-({}^1\Sigma^+)$	113.9	115.0
$B_7O_2\text{-B}^-({}^1A_1) \rightarrow B_6O\text{-A}^-({}^2A'') + BO({}^2\Sigma^+)$	111.2	111.9
$B_8O\text{-A}({}^1A_1) \rightarrow B_8({}^3A'_2) + O({}^3P)$	176.1	177.6
$B_8O\text{-B}^-({}^2A') \rightarrow B_7({}^2B_2) + BO^-({}^1\Sigma^+)$	120.2	120.5
$B_8O\text{-B}^-({}^2A') \rightarrow B_7^-({}^1A_1) + BO({}^2\Sigma^+)$	116.8	117.7
$B_8O_2\text{-A}({}^1A_1) \rightarrow B_8O\text{-A}({}^1A_1) + O({}^3P)$	171.0	172.4
$B_8O_2\text{-C}^-({}^2B_g) \rightarrow B_6({}^1A_1) + BO^-({}^1\Sigma^+) + BO({}^2\Sigma^+)$	247.7	248.7
$B_8O_2\text{-C}^-({}^2B_g) \rightarrow B_6^-({}^2B_{2g}) + 2BO({}^2\Sigma^+)$	232.6	234.1
$B_9O\text{-A}({}^2A') \rightarrow B_8({}^3A'_2) + BO({}^2\Sigma^+)$	72.8	73.2
$B_9O\text{-A}^-({}^1A') \rightarrow B_8^-({}^2B_1) + BO({}^2\Sigma^+)$	86.4	87.0
$B_9O\text{-A}^-({}^1A') \rightarrow B_8({}^3A'_2) + BO^-({}^1\Sigma^+)$	98.9	99.2
$B_9O_2\text{-A}({}^2A_2) \rightarrow B_7({}^2B_2) + 2BO({}^2\Sigma^+)$	196.4	197.1
$B_9O_2\text{-A}^-({}^1A_1) \rightarrow B_7({}^2B_2) + BO({}^2\Sigma^+) + BO^-({}^1\Sigma^+)$	245.2	246.2
$B_9O_2\text{-A}^-({}^1A_1) \rightarrow B_7^-({}^1A_1) + 2BO({}^2\Sigma^+)$	241.8	242.8
$B_{10}O\text{-A}({}^1A) \rightarrow B_{10}({}^1A_g) + O({}^3P)$	160.8	162.3
$B_{10}O\text{-B}^-({}^2A_2) \rightarrow B_9^-({}^1A_{1g}) + BO({}^2\Sigma^+)$	110.7	111.9
$B_{10}O\text{-B}^-({}^2A_2) \rightarrow B_9({}^2A_1) + BO^-({}^1\Sigma^+)$	121.3	122.3
$B_{10}O_2\text{-A}({}^1A_g) \rightarrow B_8({}^3A'_2) + 2BO({}^2\Sigma^+)$	187.3	188.3
$B_{10}O_2\text{-A}^-({}^2B_u) \rightarrow B_8({}^3A'_2) + BO({}^2\Sigma^+) + BO^-({}^1\Sigma^+)$	209.7	210.7
$B_{10}O_2\text{-A}^-({}^2B_u) \rightarrow B_8^-({}^2B_1) + 2BO({}^2\Sigma^+)$	197.2	198.5

TABLE 5: Calculated Bond Lengths, Bond Angles, and B–O Harmonic Stretching Frequencies of the BBO Units in the Lowest-Lying Boron Oxides (B3LYP/6-31G(d))

label	symmetry, state	$r(\text{B}-\text{O})$, Å	$r(\text{B}-\text{BO})$, Å	$\angle(\text{BOB})$, deg	BO stretch frequency, cm ⁻¹
B ₅ O-A	$C_{2v}, ^2\text{A}_1$	1.211	1.638	180.0	2011
B ₅ O-A ⁻	$C_{2v}, ^1\text{A}_1$	1.225	1.635	180.0	1926
B ₅ O ₂ -A	$C_s, ^2\text{A}'$	1.211	1.636	179.4	2014
B ₅ O ₂ -D	$C_{2v}, ^2\text{B}_2$	1.209	1.637	179.7	2019,2014
B ₅ O ₂ -E	$D_{\infty h}, ^2\Pi_u$	1.210	1.631	180.0	2013,2010
B ₅ O ₂ -A ⁻	$C_s, ^1\text{A}'$	1.234	1.638	179.5	1931
B ₅ O ₂ -D ⁻	$C_{2v}, ^1\text{A}_1$	1.222	1.638	179.2	1949,1938
B ₅ O ₂ -E ⁻	$D_{\infty h}, ^1\Sigma_g^+$	1.225	1.619	180.0	1937,1932
B ₆ O-A	$C_s, ^1\text{A}'$	1.211	1.640	179.7	2011
B ₆ O-A ⁻	$C_s, ^2\text{A}''$	1.227	1.616	179.8	1916
B ₆ O ₂ -A	$C_s, ^1\text{A}'$	1.211	1.637	179.5	2012
B ₆ O ₂ -B	$D_{2h}, ^1\text{A}_g$	1.210	1.636	180.0	2019,2017
B ₆ O ₂ -C	$C_s, ^1\text{A}'$	1.211	1.638	179.3	2010
B ₆ O ₂ -A ⁻	$C_s, ^2\text{A}'$	1.228	1.614	180.0	1906
B ₆ O ₂ -B ⁻	$D_{2h}, ^2\text{A}_g$	1.222	1.633	180.0	1950,1943
B ₆ O ₂ -C ⁻	$C_s, ^2\text{A}'$	1.227	1.616	179.6	1917
B ₇ O-B	$C_s, ^2\text{A}''$	1.212	1.632	179.4	2006
B ₇ O-C	$C_{2v}, ^2\text{B}_1$	1.212	1.637	180.00	2001
B ₇ O-B ⁻	$C_s, ^1\text{A}'$	1.224	1.618	179.9	1935
B ₇ O-C ⁻	$C_{2v}, ^1\text{A}_1$	1.225	1.614	180.0	1931
B ₇ O ₂ -C	$C_{2v}, ^2\text{B}_1$	1.210	1.640	179.5	2016,2014
B ₇ O ₂ -C ⁻	$C_{2v}, ^1\text{A}_1$	1.220	1.643	179.4	1950,1946
B ₈ O-B	$C_s, ^1\text{A}'$	1.212	1.633	179.3	2010
B ₈ O-B ⁻	$C_s, ^2\text{A}'$	1.222	1.626	180.0	1950
B ₈ O ₂ -B	$C_{2h}, ^1\text{A}_g$	1.210	1.638	179.6	2010,2008
B ₈ O ₂ -B ⁻	$C_{2h}, ^2\text{B}_g$	1.221	1.629	179.8	1953,1945
B ₉ O-A	$C_s, ^2\text{A}'$	1.211	1.635	179.4	2013
B ₉ O-A ⁻	$C_s, ^1\text{A}'$	1.220	1.632	179.8	1957
B ₉ O ₂ -A	$C_{2v}, ^2\text{A}_2$	1.210	1.635	179.5	2013,2011
B ₉ O ₂ -A ⁻	$C_{2v}, ^1\text{A}_1$	1.220	1.628	179.8	1964,1959
B ₁₀ O-B	$C_{2v}, ^1\text{A}_1$	1.213	1.632	180.0	2002
B ₁₀ O-C	$C_s, ^1\text{A}'$	1.211	1.637	179.5	2011
B ₁₀ O-B ⁻	$C_{2v}, ^2\text{A}_2$	1.222	1.624	180.0	1946
B ₁₀ O-C ⁻	$C_s, ^2\text{A}''$	1.222	1.625	179.9	1946
B ₁₀ O ₂ -A	$C_{2h}, ^1\text{A}_g$	1.210	1.636	179.3	2018,2016
B ₁₀ O ₂ -B	$C_{2v}, ^1\text{A}_1$	1.210	1.634	179.4	2019,2018
B ₁₀ O ₂ -A ⁻	$C_{2h}, ^2\text{B}_u$	1.219	1.633	179.6	1963,1959
B ₁₀ O ₂ -B ⁻	$C_{2v}, ^2\text{A}_1$	1.220	1.622	179.9	1960,1953

mol, and the binding of BO⁻ to a B₆ cycle is exothermic by -126.5 kcal/mol. The global adiabatic EA calculated from neutral B₇O-A and anion B₇O-B⁻ is EA(B₇O) = 3.00 eV. This is ~ 0.3 eV larger than the value of the closed-shell B₆O species (2.69 eV) but ~ 0.4 eV smaller than for the radical B₅O (3.44 eV).

We examined a variety of isomers for the dioxide B₇O₂, and the ones having relatively high symmetry shown in Figure 4 are the lowest energy structures. These include the following structures: B₇O₂-A formed from binding of the second O atom to a neighboring BB bond of B₇O-A; B₇O₂-B also formed from B₇O-A but with the additional O adding at the opposite side of the existing O along the C₂ axis; B₇O₂-C arising from the recombination of two BO radicals with a B₅ unit; B₇O₂-D derived from B₇O-D with the O bonded to the opposite end. Our G3B3 results show that there is no significant difference in energy among these four isomers. B₇O₂-A (²A₂) is predicted to be the lowest energy isomer but is only ~ 2 kcal/mol more stable than B₇O₂-C (²A₁) and B₇O₂-B (²B_{1g}). Only the isomer B₇O₂-A has been previously reported.²⁴ The two terminal BO groups of B₇O₂-C (²A₁) have the same distances and vibrational frequencies as other terminal BO groups. The binding of either two O atoms to a B₇ moiety giving B₇O₂-A or two BO radicals to a B₅ unit generating B₇O₂-C are exothermic by -346.8 and -199.4 kcal/mol, respectively.

Electron addition to the radical B₇O₂-C does not lead to significant distortion of the molecular geometry and gives rise

TABLE 6: Calculated Vertical Detachment Energies (VDEs, in eV) of the Boron Oxide Anions B_nO_m⁻ for n = 1–10, m = 1–2

anion	neutral	VDE	
		G3B3	CCSD(T)/CBS ^a
BO ⁻ (¹ S ⁺)	BO (² S ⁺)	2.61	2.56
BO ₂ ⁻ (¹ S _g ⁺)	BO ₂ (² P _g)	4.52	4.53
BOB ⁻ (² S _g ⁺)	BOB (¹ S _g ⁺)	0.10	0.03
BBO ⁻ (² Π)	BBO (¹ S ⁺)	1.56	1.53 ^b
OBBO ⁻ (² B _u)	B ₂ O ₂ (¹ S _g ⁺)	0.84	0.74
B ₃ O ⁻ (³ A ₁)	B ₃ O (⁴ Σ ⁻)	2.28	2.22
B ₃ O ₂ ⁻ (³ S _u ⁻)	B ₃ O ₂ (² P _g)	3.04	3.00
B ₄ O ⁻ (² A ₁)	B ₄ O (¹ A ₁)	2.68	2.67
B ₄ O ₂ ⁻ (² Π)	B ₄ O ₂ (³ S _g ⁻)	3.22	3.16
B ₅ O-A ⁻ (¹ A ₁)	B ₅ O-A (² A ₁)	3.60	
B ₅ O ₂ -D ⁻ (¹ A ₁)	B ₅ O ₂ -D (² B ₁)	4.63	
B ₆ O-A ⁻ (² A ^{''})	B ₆ O-A (¹ A')	2.73	
B ₆ O ₂ -B ⁻ (² A _g)	B ₆ O ₂ -B (¹ A _g)	3.63	
B ₇ O-B ⁻ (¹ A')	B ₇ O-B (² A ^{''})	3.52	
B ₇ O ₂ -B ⁻ (¹ A ₁)	B ₇ O ₂ -B (² A ₁)	3.85	
B ₈ O-B ⁻ (² A ^{''})	B ₈ O-B (¹ A')	4.09	
B ₈ O ₂ -C ⁻ (² B _g)	B ₈ O ₂ -C (¹ A _g)	4.22	
B ₉ O-A ⁻ (¹ A')	B ₉ O-A (² A')	3.87	
B ₉ O ₂ -A ⁻ (¹ A ₁)	B ₉ O ₂ -A (² A ₂)	4.81	
B ₁₀ O-B ⁻ (² A ₂)	B ₁₀ O-B (¹ A ₁)	4.39	
B ₁₀ O ₂ -A ⁻ (² B _u)	B ₁₀ O ₂ -A (¹ A _g)	3.67	

^a CCSD(T)/CBS values taken from ref 23. ^b CCSD(T)/CBS value, this work.

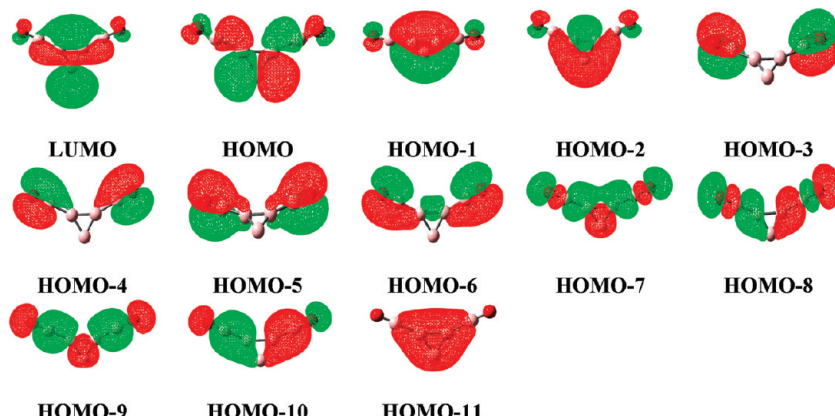


Figure 8. Molecular orbitals of the anion $B_5O_2^-$.

to the closed-shell anion $B_7O_2-C^-$ (C_{2v} , 1A_1), which is the ground state structure of the $B_7O_2^-$ anion. As for $B_6O_2^-$, the presence of the additional electron enhances the strength of the BO bonds due to electron redistribution and makes these structures more stable than alternative structures. The global adiabatic EA of B_7O_2 from B_7O_2-A and $B_7O_2-C^-$ is $EA(B_7O_2) = 3.62$ eV, even larger than the values obtained for the open-shell systems B_7O or B_5O .

B_8O , B_8O_2 , and Their Anions. The three lowest energy structures of the neutral B_8O clusters are shown in Figure 5. Our results are in agreement with the previous DFT/MD predictions²⁴ that the most stable isomer is B_8O-A (C_{2v} , 1A_1). This structure is generated from bridging an O to a BB bond at the perimeter of the most stable B_8 (C_{2v}) cluster. The low symmetry B_8O-B (C_s , $^1A'$) isomer containing one BO unit binding at the end of a B_7 ring is the next most stable isomer. Structure B_8O-C , in which O is bound to one B of the B_8 motif, is very unstable, ~ 85 kcal/mol higher in energy than B_8O-A . The higher stabilities of B_8O-A and B_8O-B are due to the presence of the B_8 and B_7 entities, even though the B_7 unit involved is again not the lowest energy isomer. Condensation of BO and B_7 leads to substantial distortion of the original B_7 geometry, and reduces the stability of the resulting isomers B_8O-B and B_8O-C . The exocyclic BO bond in B_8O-C has a longer distance of 1.266 Å and a lower stretching frequency of 1588 cm^{-1} , in contrast to the more typical values of 1.212 Å and 2010 cm^{-1} in B_8O-B .

The ELF plots for B_8O-A emphasize that each of the two V(BO) basins contains ~ 2 e, suggesting the presence of two classical single BO bonds. Each of the V(BBB) basins around the perimeter contains ~ 3 e, indicative of the emergence of two three-center bonds in the B_8 moiety. Electron populations for other basins are close to each other at ~ 2.8 e, indicating a strong electron delocalization. A similar electron delocalization is found in B_8O-B , in which the different V(BBB) basins along the B_7 perimeter contain each 2.5–2.9 e. Such a repartitioning of the density plays a crucial role in compensating for the loss of the original B_7 structure and contributes to the stabilization of isomer B_8O-B .

Both doublet and quartet spin states were considered for the anionic B_8O^- clusters. The quartets were found to be higher in energy. The energy ordering of the isomers is again found to reverse on electron attachment. Thus, B_8O-B^- ($^2A'$) becomes the global energy minimum followed by B_8O-A^- (2B_1), 3.9 kcal/mol higher in energy. The global adiabatic EA(B_8O) is 2.56 eV, a quite high value considering that B_8O is closed shell.

Geometry features of the two lowest-lying B_8O_2 isomers are summarized in Figure 5. Our extensive search for possible

atomic arrangements confirms that the neutral B_8O_2-A (1A_1) is the most stable isomer,²⁴ with the high symmetry B_8O_2-B (C_{2h} , 1A_g) isomer 21.5 kcal/mol higher in energy. Structure B_8O_2-A is generated by adding the second O atom to B_8O-A at the opposite side of the existing oxygen. B_8O_2-B is derived by binding two BO radicals to two diagonal B centers of a B_6 (C_{2h}) ring. All other alternative structures are ~ 38 kcal/mol higher in energy.

Similar to B_5O , B_5O_2 , B_6O , B_6O_2 , B_7O , and B_7O_2 , the relative energy ordering is again reversed in the anion. Structure $B_8O_2-B^-$ (C_{2h} , 2B_g) is now the most stable anionic isomer. Consistently, the most stable anionic clusters of boron oxides and dioxides contain one or two exocyclic BO groups. The global adiabatic EA(B_8O_2) is 3.19 eV calculated from the singlet neutral B_8O_2-A and the doublet anion $B_8O_2-B^-$.

B_9O , B_9O_2 , and Their Anions. Extensive exploration on the potential energy surface of the monoxide isomers for B_9O resulted in the three structures displayed in Figure 8, and these isomers are in agreement with the DFT/MD search of Drummond et al.²⁴ Our calculations also agree that the B_9O-A (C_s , $^2A'$), in which one BO binds in the plane of a cyclic B_8 unit, is the most stable isomer. Structure B_9O-B involving a bond of O with two B atoms of a B_9 (D_{2h}) ring is only 7.5 kcal/mol higher, even though the B_9 moiety present in the monoxide is again not the most favored isomer for the pure boron cluster. Isomer B_9O-C (C_{2v} , 2B_2) involves incorporation of one BBO group to a B_7 unit, and is 13.5 kcal/mol higher in energy than B_9O-A . Again, the BO terminal group of B_9O-A has a typical terminal bond distance and stretching frequency.

For the anion of B_9O , we predict no reversal of relative energy ordering of the isomers following electron attachment, even though the singlet B_9O-C^- (C_{2v} , 1A_1) is substantially stabilized. B_9O-A^- (C_s , $^1A'$) remains the preferred isomer for the anion, but is now only 2.7 kcal/mol more stable than B_9O-C^- . As in many of the other clusters, the geometries of the anions are very similar to those of the corresponding neutrals. The global adiabatic EA(B_9O) of 3.70 eV for neutral B_9O-A is relatively high for the series of boron monoxides (Table 4).

The dioxide B_9O_2 has not been considered in previous studies. We optimized a large number of structures at the B3LYP/6-31G(d) level and refined the energies of the three lowest-lying structures by G3B3 calculations (Figure 6). Isomer B_9O_2-A (C_{2v} , 2B_2) is the most stable. Although structure B_9O_2-B (C_s , $^2A'$) is made from the most stable monoxide B_9O-A by addition of O at the opposite side of the existing BO, it is 10.0 kcal/mol higher in energy. The other isomers, including the high symmetry B_9O_2-C isomer, are >30 kcal/mol higher in energy than B_9O_2-A . The geometry of the global minimum B_9O_2-A , which consists

of two BO units bonding with a B₇ ring in either the neutral or anionic state, is analogous to that of the boron hydride B₇H₂⁻ and doped B₇Au₂⁻ cluster.⁴⁴ The boronyl group behaves as a substituent and can be used to replace the hydrogen atom. The BO group should possess a chemical effect similar to the isoelectronic cyano (CN) substituent.⁷

Following electron attachment, the B₉O₂-A⁻ isomer remains as the global minimum for the dioxide anion with an adiabatic EA(B₉O₂) = 4.69 eV.

B₁₀O, B₁₀O₂, and Their Anions. The B₁₀O clusters can be generated either by attaching one O atom onto the most stable B₁₀ ring to generate B₁₀O-A (¹A), or by binding a BO group to a B₉ ring giving structures B₁₀O-B (C_{2v} , ¹A₁) and B₁₀O-C (C_s , ¹A') (Figure 7). B₁₀O-A is by far the favored isomer, and is 21.3 and 23.5 kcal/mol more stable than B₁₀O-B and B₁₀O-C, respectively.

The general feature of the monoxides that the energy ordering of isomers is changed in the anion, is again found for B₁₀O⁻. Structure B₁₀O-B⁻ (C_{2v} , ²A₂) is now the lowest energy anion isomer. Reaction energies show that the decomposition of B₁₀O-B⁻ → BO⁻ + B₉ (ΔH_r = 121.3 kcal/mol) is more energy demanding than its fragmentation giving BO + B₉⁻ (ΔH_r = 110.7 kcal/mol), consistent with the difference in the EAs of the fragments. The global adiabatic EA(B₁₀O) of 3.36 eV is larger than EA(B₈O) and EA(B₆O) (Table 3).

Following a geometry search for both neutral and anionic B₁₀O₂ clusters, the three lowest-lying isomers are shown in Figure 7. B₁₀O₂-A, which is generated from addition of BO to B₁₀O-C, is the global equilibrium structure for both the neutral (C_{2h} , ¹A_g) and the anion (C_{2h} , ²B_u). Neutral B₁₀O₂-C (C_{2v} , ¹A₁) is 3.8 kcal/mol higher in energy than B₁₀O₂-A, and the anion B₁₀O₂-B⁻ (C_{2v} , ²A₁) is 14.2 kcal/mol less stable than B₁₀O₂-A⁻. The adiabatic EA(B₁₀O₂) is 3.54 eV, the largest value for dioxides with an even number of electrons. This demonstrates the ability of the larger B_n boron skeleton to receive and redistribute the excess electron, thereby increasing the stability of the resulting anion.

Bond Character of the Boronyl Groups. All of the lowest energy isomers for the anionic monoxides B_nO⁻ contain a boronyl BO bonded to a B_{n-1} unit, whereas the global minima of the anionic dioxides B_nO₂⁻ are usually composed of two boronyl groups attached to a B_{n-2} moiety. We previously showed²³ that the best combination arises when a BO bond and a boron cycle can be simultaneously formed, as in the cases of B₄O and B₄O₂. To provide further insight, the canonical molecular orbitals (CMOs) of the global minima for B_nO₂⁻ (n = 5–10) were examined. An NBO analysis reveals that a consistent set of six MOs in each of the dioxides is responsible for the bonding of the BO groups. As an example, Figure 8 displays the MOs of the B₅O₂⁻ anion. The HOMO-3, HOMO-4, HOMO-5, HOMO-6, HOMO-12, and HOMO-13 correspond to the BO units. Two of these molecular orbitals (HOMO-12 and HOMO-13) are low-energy BO σ -orbitals, and the four remaining MOs are responsible for formation of two π BO bonds. Table 5 summarizes the bond distances and stretching frequencies of the boron oxides. The BO distances of the anions fall within a small range from 1.219 to 1.222 Å. The BO stretch frequencies vary within the range 1920–2020 cm⁻¹. Thus, the strength of the BO bond plays a predominant role in the high stability of the anions.

Electron Delocalization and Aromaticity. Bare boron clusters have been suggested to be highly aromatic systems with mostly planar, high symmetry structures.² We now describe how oxidation of boron clusters forming boron oxides could affect

the electron distribution. We consider in some detail the simplest case of the B₅O₂⁻ clusters whose CMOs are shown in Figure 8. The NBO analysis shows that the five orbitals (HOMO, HOMO-2, HOMO-7, HOMO-10, and HOMO-11) are localized into five two-electron–two-center bonds (three orbitals are responsible for three 2e–2c bonds of B₃⁻, and two orbitals are responsible for bonding between BO groups and B₃⁻). The HOMO-1 is a global π -bonding MO consistent with B₅O₂⁻ having π -aromaticity. The HOMO-8 and HOMO-9 are local σ -bonding MOs, but these result in a σ -antiaromatic character for B₅O₂⁻. Such a conflicting aromaticity will reduce the aromaticity of the three-membered boron ring.

Although neutral B₆O₂-B (D_{2h}) is 6.7 kcal/mol less stable than the global minimum B₆O₂-A, the anion B₆O₂-B⁻ (D_{2h}) becomes a global minimum with an energy of ~30 kcal/mol lower than the next low-lying isomer, and ~44 kcal/mol lower than the anion B₆O₂-A⁻. To probe this change in energy ordering, an NBO analysis of the neutral B₆O₂ (D_{2h}) was performed and compared to the MOs of the relevant derivatives such as B₄ (D_{2h}) and B₄H₂ (D_{2h}) in their most stable forms. As shown in Figure 9, there is an analogy between the MOs of B₄, B₄H₂, and B₆O₂ (D_{2h}). Four MOs of the B₄ (HOMO-1, HOMO-3, HOMO-4, and HOMO-5) are responsible for the four peripheral 2e–2c bonds. The HOMO-2 and HOMO are the π - and σ -MOs, respectively, which leads to assignment of a doubly aromatic character for B₄. There are six 2e–2c bonds in B₄H₂ and B₆O₂ (four corresponding to four bonds in B₄, and two corresponding to either two B–H bonds in B₄H₂ or two B–BO bonds in B₆O₂), formed from six MOs in each system (HOMO, HOMO-2, HOMO-3, HOMO-4, HOMO-5, and HOMO-6 for B₄H₂; HOMO, HOMO-6, HOMO-7, HOMO-10, HOMO-11, and HOMO-12 for B₆O₂). Only the remaining HOMO-1 in B₄H₂ is a π -orbital which makes the B₄H₂ (D_{2h}) species aromatic and the global energy minimum. For the B₆O₂ (D_{2h}), the HOMO-1 is a global π -orbital, and the two remaining HOMO-8 and HOMO-9 are global σ -orbitals. There is however a remarkable difference when adding either H atoms or BO groups to the bare boron B₄. Introduction of two H atoms to the system decreases the delocalized σ -electrons, and addition of two BO groups increases the delocalized σ -electrons. Consequently, the B₆O₂ (D_{2h}) bears two delocalized π -electrons and four delocalized σ -electrons. Following addition of two electrons to the LUMO of B₆O₂, the dianion B₆O₂²⁻ now possesses six delocalized σ -electrons and two delocalized π -electrons, and becomes a doubly (π and σ) aromatic species. This is consistent with neutral B₆O₂-B being a higher energy isomer and the anion B₆O₂-B⁻ being the global minimum.

Similar NBO analyses were performed for the larger anions B_nO₂⁻. The MOs responsible for electron delocalization and aromaticity are shown in Figure 10. B₇O₂⁻ is a doubly (π and σ) aromatic system with two delocalized π -electrons and six delocalized σ -electrons. In contrast, B₈O₂⁻ and B₉O₂⁻ are suggested to be π -antiaromatic (four delocalized π -electrons) and σ -aromatic (six delocalized σ -electrons).

Topological Analysis of Electron Densities. A topological analysis of electron densities is performed by the ELF technique, which is a useful approach for the analysis of the bonding,²³ aromaticity,^{45,46} and electron delocalization⁴⁷ in a compound. Evaluation of aromaticity can be done using the bifurcation values of the components ELF _{σ} and ELF _{π} obtained separately from the total densities; a high bifurcation value of either ELF _{σ} or ELF _{π} indicates a good electron delocalization.

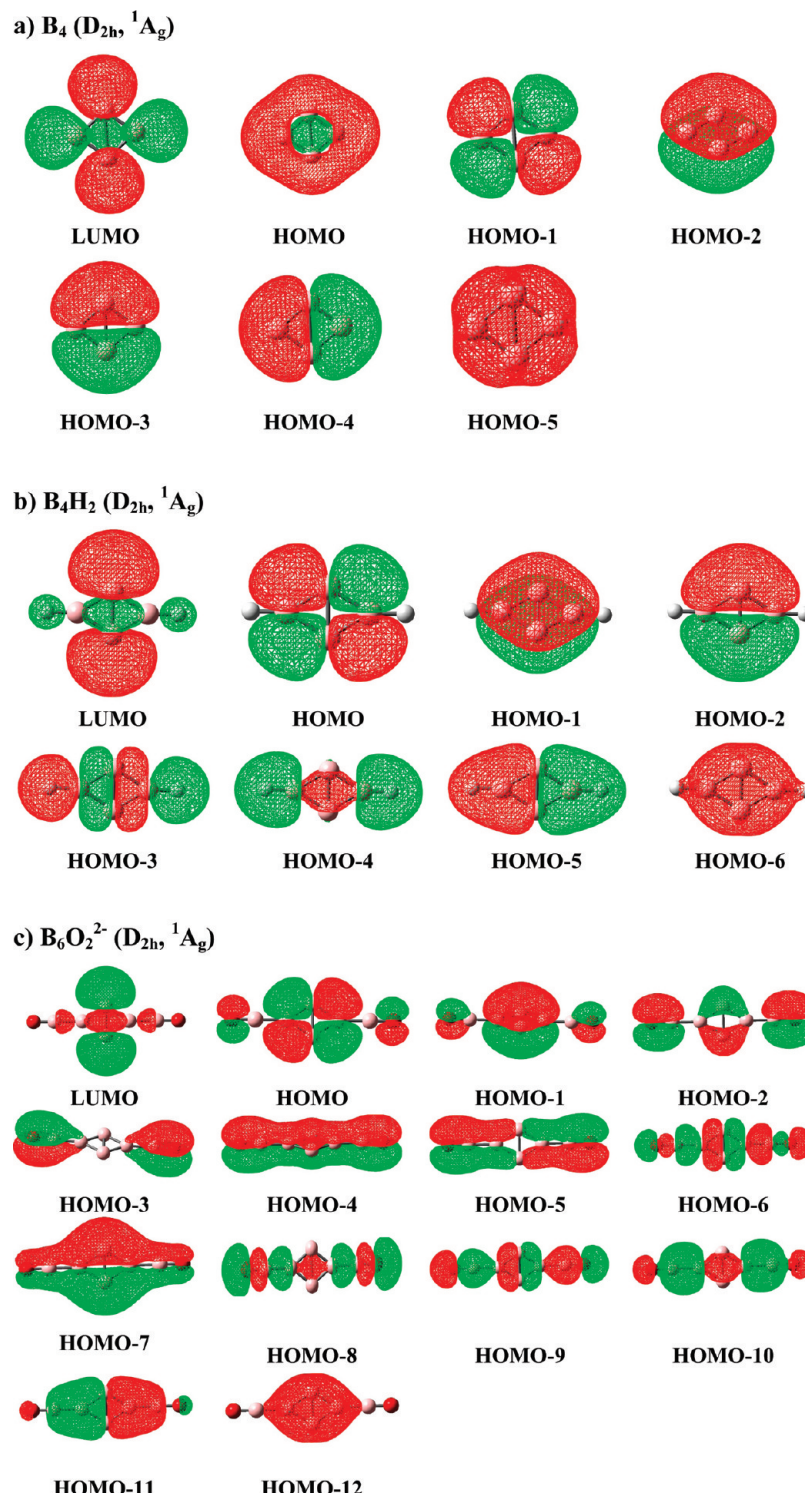


Figure 9. Molecular orbitals of (a) B_4^{2-} (D_{2h} , 1A_g), (b) $B_4H_2^{2-}$ (D_{2h} , 1A_g), and (c) $B_6O_2^{2-}$ (D_{2h} , 1A_g).

The total ELFs of the boron dioxide anions at their bifurcations are illustrated in Figure 11. The electron distributions around the B–O and the B–BO bonds in all systems are similar to each other. Each of the V(B,O) basins contains $\sim 3.4\text{--}3.5$ e, and the population in each V(B,BO) basin is ~ 2.4 e. The remaining basins are perfectly delocalized in local rings containing $(n - 2)$ B atoms (i.e., a three-membered ring for $B_5O_2^-$, a four-membered ring for $B_6O_2^-$, etc.), which is consistent with a high thermodynamic stability for the anions. The electron populations of the total ELF also

confirm the presence of multicenter bonds, which are a typical feature in boron compounds.⁴⁸ The anion $B_7O_2^-$ possesses three multielectron–three-center bonds in which each of the V(B,B,B) basins contains ~ 2.8 e. Similar observations can be made for $B_8O_2^-$, $B_9O_2^-$, and $B_{10}O_2^-$, which have four, five, and six multiple bonds, respectively. Overall, the inherent features of pure boron clusters such as planarity, strong electron delocalization, aromaticity, and multicenter bonds remain the essential characteristics of the boron oxide anions.

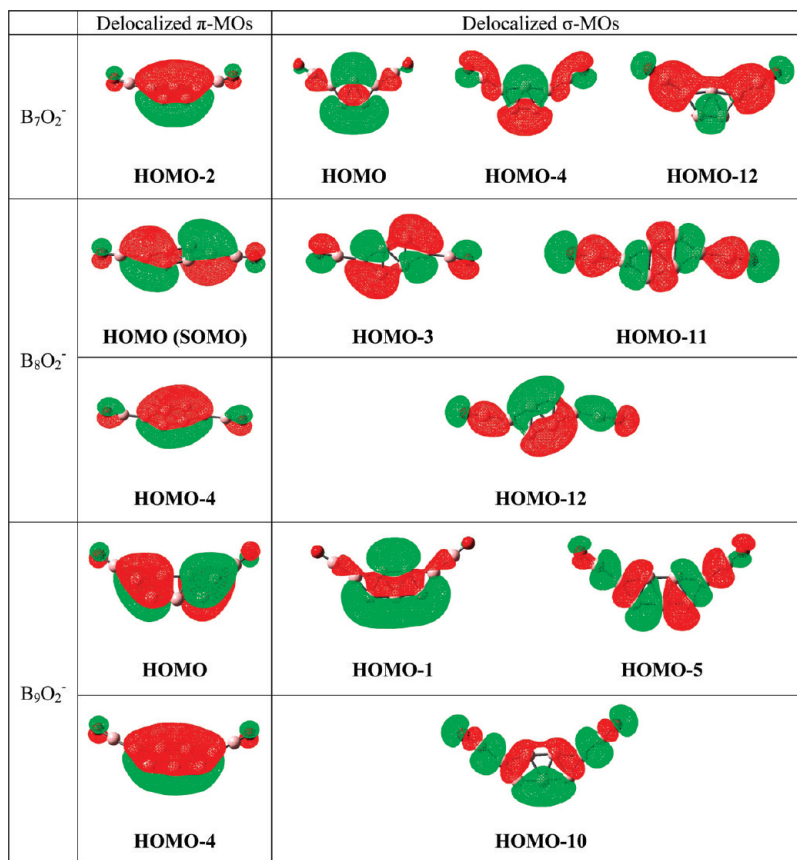


Figure 10. Selected molecular orbitals relevant to the delocalized σ - and π -electrons in some dioxide anions.

Stability, Binding Energy, and Resonance Energy. To probe further the stability of the anions with respect to electron removal, we calculated the vertical electron detachment energies (VDEs) using the G3B3 method (Table 6). The VDEs are not significantly larger than the global adiabatic EAs of the neutrals stated above. The size dependence of the EAs is illustrated in Figure 12. Except for the B_2 species, all of the oxides possess EAs > 2 eV, with B_5O_2 having the largest EA. Beginning with B_4 , there is a moderate odd–even alternation in both monoxide and dioxide series.

The relative stabilities of the clusters B_nO_m ($n = 1–10$ and $m = 0, 1$, and 2) can be evaluated in terms of the average binding energy (E_b , defined as the normalized binding energy per atom)

$$E_b = [nE(B) + mE(O) - E(B_nO_m)]/(n + m) \quad (1)$$

and the second-order difference in the total energy (Δ^2E), defined as follows:

$$\Delta^2E(B_nO_m) = E(B_{n-1}O_m) + E(B_{n+1}O_m) - 2E(B_nO_m) \quad (2)$$

The average binding energies E_b 's of the pure B_n and oxide B_nO_m clusters for both neutral and anions are compared in Figures 13 and 14, respectively. The binding energy is increased when oxygen is added to a boron cluster forming BO bonds. For the same total number of atoms, the E_b of B_2O_2 is higher than the E_b of B_2O and B_2 . The binding energy of B_2O_2 is remarkably high for the neutrals; the additional stability of B_2O_2

is also found in Δ^2E (Figure 15). The plots for the anions (Figure 14) show that BO^- and BO_2^- have E_b values > 0.5 eV larger than the values for the other oxides.

In our previous study,²³ we considered the resonance energy (RE)⁴⁹ of a boron cluster⁵⁰ defined by eq 3:

$$RE(B_n) = \Delta E(B_n \rightarrow nB) - x\Delta E(B_2 \rightarrow nB) \quad (3)$$

in which the diatomic B_2 can be in either the ${}^1\Sigma_g^+$ or the ${}^3\Sigma_g^-$ state, and x is the number of BB bonds in B_n . In a similar way, we can define the REs of the neutral and anion boron oxides as expressed in eqs 4 and 5, respectively:

$$RE(B_nO_m) = \Delta E(B_nO_m \rightarrow nB + mO) - x\Delta E(B_2({}^1\Sigma_g^+) \rightarrow 2B) - m\Delta E(BO({}^2\Sigma^+) \rightarrow B + O) \quad (4)$$

$$RE(B_nO_m^-) = \Delta E(B_nO_m^- \rightarrow nB + mO) - (x - 1)\Delta E(B_2({}^1\Sigma_g^+) \rightarrow 2B) - \Delta E(B_2({}^4\Sigma_g^-) \rightarrow 2B + e) - m\Delta E(BO({}^2\Sigma^+) \rightarrow B + O) \quad (5)$$

where n is the number of B atoms, $m = 1$ for monoxides, $m = 2$ for dioxides, and similarly x is the number of BB bonds. The normalized resonance energy (NRE) is defined as $RE/(n + m)$. To facilitate the comparison, we consider the same value of x for each series of n . We initially analyzed²³ the resonance energies of the boron clusters up to $n = 4$ using the approach⁵⁰ employed for analyzing the Al_n clusters for up to $n = 4$. In this approach, we counted only the number of delocalized π -elec-

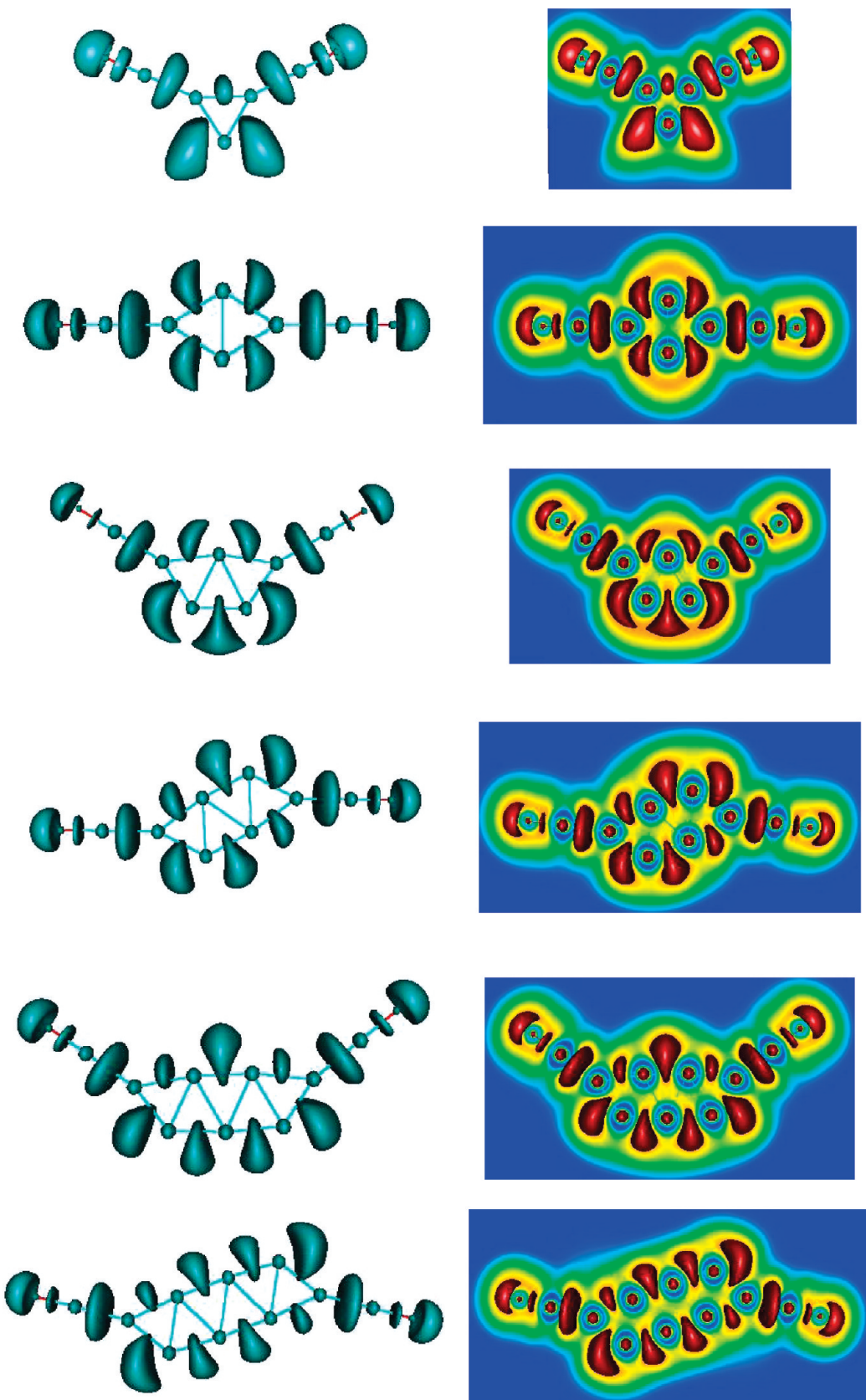


Figure 11. ELF plots for boron dioxide anions $B_nO_m^-$ ($n = 5–10$ and $m = 1–2$).

trons, so for B_4^{2-} we used $x = 3$. In our subsequent study of the larger boron clusters,⁴³ use of only the delocalized electrons would have led to unreasonably large resonance energies, and as discussed previously, it is difficult to determine how many delocalized electrons should be counted. As the reference model

for predicting the resonance energy is somewhat arbitrary,^{51,52} we chose to use the total number of BB bonds in a cluster in our resonance energy estimates for the pure boron clusters.⁴³ We thus use the singlet state for B_2 (${}^1\Sigma_g^+$) as the energy of a bond. For B_3 , $x = 3$, whereas for B_4 , $x = 5$, and for B_5 , $x = 7$,

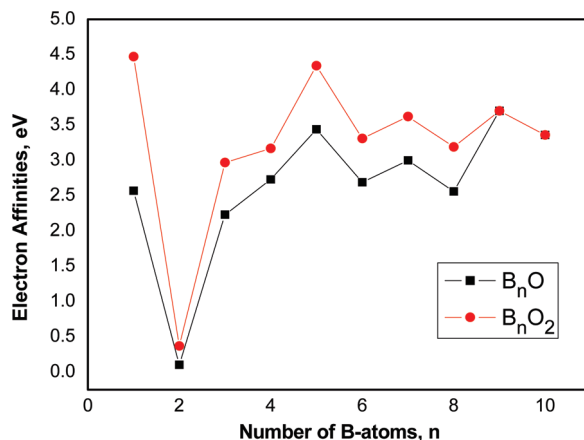


Figure 12. Size dependence of the adiabatic electron affinities (EAs) of B_nO and B_nO_2 clusters.

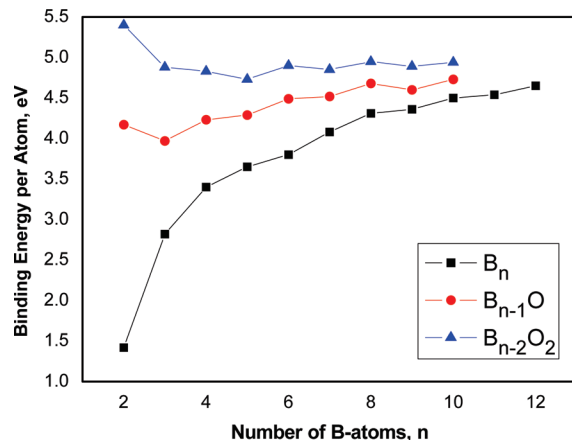


Figure 13. Size dependence of the binding energy per atom of the neutrals B_n , $B_{n-1}O$, and $B_{n-2}O_2$.

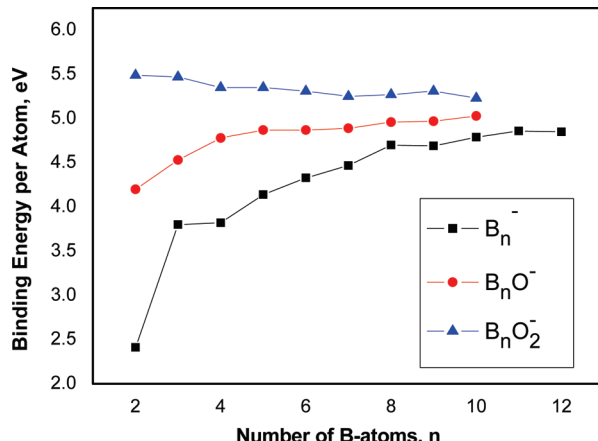


Figure 14. Size dependence of the binding energy per atom of the anions B_n^- , B_nO^- , and $B_nO_2^-$.

with the values for B_4 and B_5 coming from our analysis of the structures including the electron density analysis.⁴³ For example, B_4 is a trapezoid, so there is one B–B bond across the center which we include in addition to the four B–B bonds around the perimeter; B_5 has five perimeter BB bonds and two in the center of the cluster, giving $x = 7$. For the larger clusters, a count for effective BB bonds becomes more difficult.⁴³ For B_6 , there are arguments as to whether to assign x to either 8 or 9. The values of x and the calculated values for REs and NREs are given in the Supporting Information. Figures 16 and 17 illustrate the variation of both quantities as a function of n . The

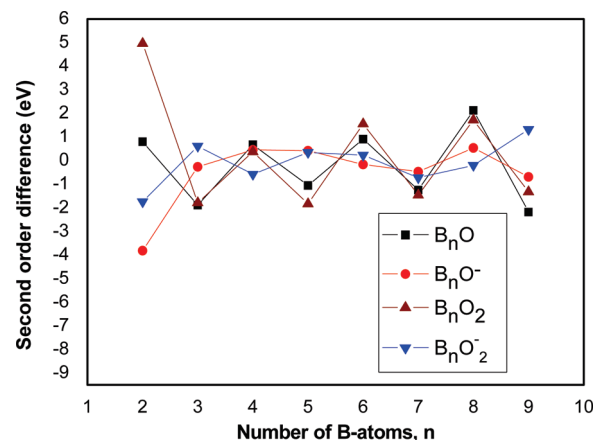


Figure 15. Second-order energy differences of the B_nO_m species.

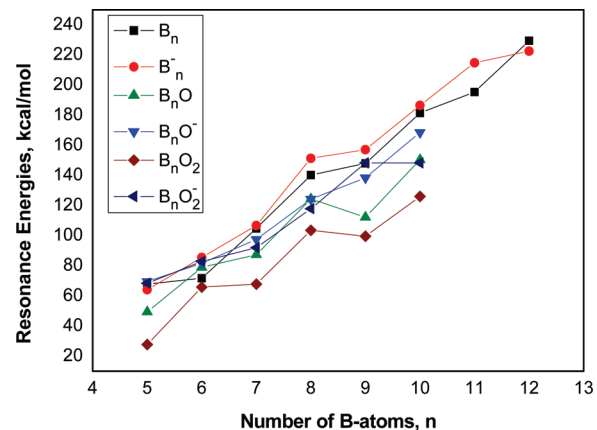


Figure 16. Resonance energies (REs, kcal/mol) of B_nO_m and $B_nO_m^-$ clusters ($n = 5 - 10$, $m = 0, 1, 2$).

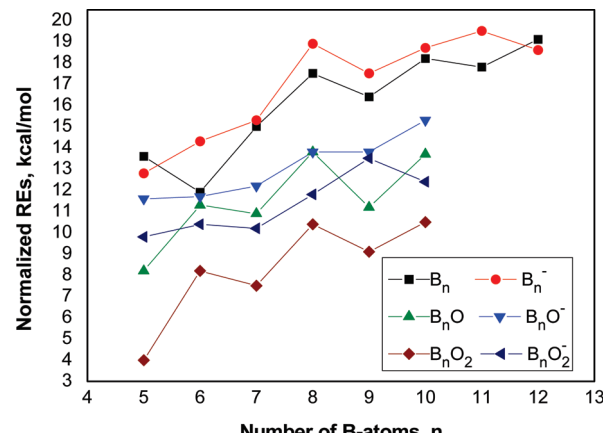


Figure 17. Normalized resonance energies (NREs) of B_nO_m and $B_nO_m^-$ clusters ($n = 5 - 10$, $m = 0, 1, 2$).

REs of the anions tend to be larger than those of the corresponding neutrals. Compared with the B_n counterparts, addition of O atoms decreases the REs. The same trend is also observed for the NREs. Thus, the BO groups act as electron-withdrawing substituents reducing the electron delocalization, and thereby the resonance energies. The reduction of the NRE amounts to 2–8 kcal/mol in going from a B_n to a B_nO_2 , in which the larger the cluster (n), the larger the reduction. However, the BO groups that are formed following oxidation of boron clusters contribute in many ways to the stability of the whole system, even though they apparently reduce the resonance energy.

Conclusion

We explored the most stable molecular structures of a series of small boron monoxide and dioxide clusters in both neutral and anionic states. We predicted their enthalpies of formation, electron affinities, vertical detachment energies, and energies for different fragmentation processes. The G3B3 method predicted results in good agreement with available experimental and more accurate theoretical values. The deviations of the G3B3 results with respect to the more accurate CCSD(T)/CBS values are, on average, ± 1.5 kcal/mol for enthalpies of formation and ± 0.03 eV for electron affinities.

The present results extend the observations we have recently made on the growth mechanism of boron oxide clusters,²³ and can be summarized as follows: (i) In each oxide, the low spin state is consistently favored over the corresponding high spin state. (ii) For neutral clusters, the most stable structure for a boron monoxide B_nO tends to be built up either by condensing the O atom on a BB edge of the B_n cycle (for B_5O , B_7O , and B_8O), or by binding one boronyl (BO) group to the B_{n-1} ring (for B_4O , B_6O , B_9O , and $B_{10}O$). The balance between the two factors is likely determined by the inherent stability of the boron cycle. (iii) A boron dioxide cluster is formed by incorporating the second O atom to the most stable form of the corresponding monoxide, with one (or two) B atom(s) at the opposite side of the first O atom (except for B_7O_2). The balance between the ring stability and the BO bond strength is again a determining factor. (iv) The anionic $B_nO_m^-$ clusters prefer to form exocyclic BO groups bound to either the B_{n-1} (for boron monoxides) or B_{n-2} (for boron dioxides) rings. This motif becomes the preferred geometric feature of the larger size boron dioxides, even in the neutral state (for B_9O_2 and $B_{10}O_2$), in such a way that a boron oxide anion $B_nO_m^-$ can be described as $B_{n-2}(BO)_2^-$. (v) There is a similarity between boron hydrides B_nH_2 and boron oxides $B_n(BO)_2$. The boronyl group behaves as an electron-withdrawing group. (vi) The boron oxides possess some of the inherent electronic properties of the parent boron clusters, such as planar geometries and multiple aromaticity. Nevertheless, the presence of O atoms significantly reduces the average energy per atom and resonance energy of the boron oxides.

Acknowledgment. Funding provided in part by the Department of Energy, Office of Energy Efficiency and Renewable Energy under the Hydrogen Storage Grand Challenge, Solicitation No. DE-PS36-03GO93013. This work was done as part of the Chemical Hydrogen Storage Center. D.A.D. is indebted to the Robert Ramsay Endowment of the University of Alabama. M.T.N. is indebted to the K. U. Leuven Research Council for support (GOA, IDO, and IUAP programs). T.B.T. thanks the Arenberg Doctoral School for a scholarship.

Note Added after ASAP Publication. This article was published ASAP on January 29, 2010, with an error in Figure 8. The correct version was reposted on February 5, 2010.

Supporting Information Available: Tables containing the total G3B3 energies, calculated resonance energies (REs), and normalized resonance energies (NREs) in kcal/mol of the B_nO_m and $B_nO_m^-$ clusters ($n = 5–10$, $m = 1–2$) as a function of the number of BB bonds (x); Cartesian coordinates for all optimized geometries; and ELF diagrams for B_nO , B_nO^- , and B_nO_2 . This material is available free of charge via the Internet at <http://pubs.acs.org>.

References and Notes

- (1) (a) Hintz, P. A.; Ruatta, S. A.; Anderson, S. L. *J. Chem. Phys.* **1990**, *92*, 292. (b) Hanley, L.; Anderson, S. L. *J. Chem. Phys.* **1988**, *89*, 2848. (c) Hintz, P. A.; Ruatta, S. A.; Anderson, S. L. *J. Chem. Phys.* **1991**, *94*, 6446. (d) Smolannoff, J.; Lapicki, A.; Kline, N.; Anderson, S. L. *J. Phys. Chem.* **1995**, *99*, 16276. (e) Peiris, D.; Lapicki, A.; Anderson, S. L.; Napora, R.; Linder, D.; Page, M. *J. Phys. Chem. A* **1997**, *101*, 9935. (f) Lapicki, A.; Peiris, D.; Anderson, S. L. *J. Phys. Chem. A* **1999**, *103*, 226.
- (2) (a) Zhai, H. J.; Kiran, B.; Li, J.; Wang, L. S. *Nat. Mater.* **2003**, *2*, 827. (b) Zhai, H. J.; Alexandrova, A. N.; Birch, K. A.; Boldyrev, A. I.; Wang, L. S. *Angew. Chem., Int. Ed.* **2003**, *42*, 6004. (c) Alexandrova, A. N.; Boldyrev, A. I.; Zhai, H. J.; Wang, L. S. *Coord. Chem. Rev.* **2006**, *250*, 2811, and references therein.
- (3) Quandt, A.; Boustani, I. *ChemPhysChem* **2006**, *6*, 2001.
- (4) (a) Gopukumar, G.; Nguyen, M. T.; Ceulemans, A. *Chem. Phys. Lett.* **2008**, *450*, 175. (b) Ceulemans, A.; Tshishimbi Muya, J.; Gopukumar, G.; Nguyen, M. T. *Chem. Phys. Lett.* **2008**, *461*, 226.
- (5) Chen, C.; He, D.; Kou, Z.; Peng, F.; Yao, L.; Yu, R.; Bi, Y. *Adv. Mater.* **2007**, *19*, 4288.
- (6) (a) Zhai, H. J.; Li, S. D.; Wang, L. S. *J. Am. Chem. Soc.* **2007**, *129*, 9254. (b) Li, S. D.; Zhai, H. J.; Wang, L. S. *J. Am. Chem. Soc.* **2008**, *130*, 2573.
- (7) Nguyen, M. T.; Ruelle, P.; Ha, T. K. *J. Mol. Struct. (THEOCHEM)* **1983**, *104*, 353, and references therein.
- (8) Nguyen, M. T. *Mol. Phys.* **1986**, *58*, 655.
- (9) Gupta, A.; Tossell, J. A. *Am. Mineral.* **1983**, *68*, 989.
- (10) Mains, G. J. *J. Phys. Chem.* **1991**, *95*, 5089.
- (11) Martin, J. M. L.; Francois, J. P.; Gijbels, R. *Chem. Phys. Lett.* **1992**, *193*, 243.
- (12) Brommer, M.; Rosmus, P. *J. Chem. Phys.* **1993**, *98*, 7746.
- (13) Ortiz, J. V. *J. Chem. Phys.* **1993**, *99*, 6727.
- (14) Neumukhin, A. V.; Weinhold, F. *J. Chem. Phys.* **1993**, *98*, 1329.
- (15) Neumukhin, A. V.; Serebrennikov, L. V. *Russ. Chem. Rev.* **1993**, *62*, 527.
- (16) Chen, K.; Lee, K.; Chang, J.; Sung, C.; Chung, T.; Liu, T.; Perng, H. *J. Phys. Chem.* **1996**, *100*, 488.
- (17) Papakondylis, A.; Mavridis, A. *J. Phys. Chem. A* **1999**, *103*, 9359.
- (18) (a) Grein, F. *J. Phys. Chem. A* **2005**, *109*, 9270. (b) Grein, F. *Chem. Phys. Lett.* **2006**, *418*, 100.
- (19) Islam, M. M.; Bredow, T.; Minot, C. *Chem. Phys. Lett.* **2006**, *418*, 565.
- (20) Liakoc, D. G.; Simandiras, E. D. *J. Phys. Chem. A* **2008**, *112*, 7881.
- (21) Chin, C. H.; Mebel, A. M.; Hwang, D. Y. *J. Phys. Chem. A* **2004**, *108*, 473.
- (22) Yao, W. Z.; Guo, J. C.; Lu, H. G.; Li, S. D. *J. Phys. Chem. A* **2009**, *113*, 2561.
- (23) Nguyen, M. T.; Matus, M. H.; Ngan, V. T.; Grant, D. J.; Dixon, D. A. *J. Phys. Chem. A* **2009**, *113*, 4895.
- (24) Drummond, M. L.; Meunier, V.; Sumpter, B. G. *J. Phys. Chem. A* **2007**, *111*, 6539.
- (25) Feng, X. J.; Luo, Y. H.; Liang, X.; Zhao, X. Z.; Cao, T. T. *J. Cluster Sci.* **2008**, *19*, 421.
- (26) (a) Curtiss, L. A.; Raghavachari, K.; Redfern, P. C.; Rassolov, V.; Pople, J. A. *J. Chem. Phys.* **1998**, *109*, 7764. (b) Baboul, A. G.; Curtiss, L. A.; Redfern, P. C. *J. Chem. Phys.* **1999**, *110*, 7650.
- (27) Becke, A.; Edgecombe, K. *J. Chem. Phys.* **1990**, *92*, 5397.
- (28) Frisch, M. J.; Trucks, G. W.; Schlegel, H. B.; Scuseria, G. E.; Robb, M. A.; Cheeseman, J. R.; Montgomery, J. A., Jr.; Vreven, T.; Kudin, K. N.; Burant, J. C.; Millam, J. M.; Iyengar, S. S.; Tomasi, J.; Barone, V.; Mennucci, B.; Cossi, M.; Scalmani, G.; Rega, N.; Petersson, G. A.; Nakatsuji, H.; Hada, M.; Ehara, M.; Toyota, K.; Fukuda, R.; Hasegawa, J.; Ishida, M.; Nakajima, T.; Honda, Y.; Kitao, O.; Nakai, H.; Klene, M.; Li, X.; Knox, J. E.; Hratchian, H. P.; Cross, J. B.; Bakken, V.; Adamo, C.; Jaramillo, J.; Gomperts, R.; Stratmann, R. E.; Yazyev, O.; Austin, A. J.; Cammi, R.; Pomelli, C.; Ochterski, J. W.; Ayala, P. Y.; Morokuma, K.; Voth, G. A.; Salvador, P.; Dannenberg, J. J.; Zakrzewski, V. G.; Dapprich, S.; Daniels, A. D.; Strain, M. C.; Farkas, O.; Malick, D. K.; Rabuck, A. D.; Raghavachari, K.; Foresman, J. B.; Ortiz, J. V.; Cui, Q.; Baboul, A. G.; Clifford, S.; Cioslowski, J.; Stefanov, B. B.; Liu, G.; Liashenko, A.; Piskorz, P.; Komaromi, I.; Martin, R. L.; Fox, D. J.; Keith, T.; Al-Laham, M. A.; Peng, C. Y.; Nanayakkara, A.; Challacombe, M.; Gill, P. M. W.; Johnson, B.; Chen, W.; Wong, M. W.; Gonzalez, C.; Pople, J. A. *Gaussian 03*, Revision C.01; Gaussian, Inc.: Wallingford, CT, 2004.
- (29) (a) Peterson, K. A.; Xantheas, S. S.; Dixon, D. A.; Dunning, T. H., Jr. *J. Phys. Chem. A* **1998**, *102*, 2449. (b) Feller, D.; Peterson, K. A. *J. Chem. Phys.* **1998**, *108*, 154. (c) Dixon, D. A.; Feller, D. *J. Phys. Chem. A* **1998**, *102*, 8209. (d) Feller, D.; Peterson, K. A. *J. Chem. Phys.* **1999**, *110*, 8384. (e) Feller, D.; Dixon, D. A. *J. Phys. Chem. A* **1999**, *103*, 6413. (f) Feller, D. *J. Chem. Phys.* **1999**, *111*, 4373. (g) Feller, D.; Dixon, D. A. *J. Phys. Chem. A* **2000**, *104*, 3048. (h) Feller, D.; Sordo, J. A. *J. Chem. Phys.* **2000**, *113*, 485. (i) Feller, D.; Dixon, D. A. *J. Chem. Phys.* **2001**, *115*, 3484. (j) Dixon, D. A.; Feller, D.; Sandrone, G. *J. Phys. Chem. A* **1999**, *103*, 4744. (k) Ruscic, B.; Wagner, A. F.; Harding, L. B.; Asher, R. L.; Feller, D.; Dixon, D. A.; Peterson, K. A.; Song, Y.; Qian, X.; Ng, C.; Liu, J.; Chen, W.; Schwenke, D. W. *J. Phys. Chem. A* **2002**, *106*, 2727. (l) Feller, D.,

- Dixon, D. A.; Peterson, K. A. *J. Phys. Chem. A* **1998**, *102*, 7053. (m) Dixon, D. A.; Feller, D.; Peterson, K. A. *J. Chem. Phys.* **2001**, *115*, 2576.
(30) Karton, A.; Martin, J. M. L. *J. Phys. Chem. A* **2007**, *111*, 5936.
(31) Chase, M. W. *J. Phys. Chem. Ref. Data, Monogr.* **1998**, *9* (Suppl. 1), 1–957.
(32) Feller, D.; Peterson, K. A.; Dixon, D. A. *J. Chem. Phys.* **2008**, *129*, 204105.
(33) Curtiss, L. A.; Raghavachari, K.; Redfern, P. C.; Pople, J. A. *J. Chem. Phys.* **1997**, *106*, 1063.
(34) Parr, R. G.; Yang, W. *Density-Functional Theory of Atoms and Molecules*; Oxford University Press: Oxford, 1989.
(35) Becke, A. D. *J. Chem. Phys.* **1993**, *98*, 5648.
(36) Frisch, M. J.; Pople, J. A.; Binkley, J. S. *J. Chem. Phys.* **1984**, *80*, 3265.
(37) (a) Silvi, B.; Savin, A. *Nature* **1994**, *371*, 683. (b) Savin, A.; Becke, A.; Flad, D.; Nesper, R.; Preuss, H.; Schnerring, H. V. *Angew. Chem., Int. Ed.* **1991**, *30*, 409. (c) Savin, A.; Silvi, B.; Colonna, F. *Can. J. Chem.* **1996**, *74*, 1088.
(38) (a) Noury, S.; Krokidis, X.; Fuster, F.; Silvi, B. *TOPMOD Package*; Universite Pierre et Marie Curie: Paris, 1997. (b) Noury, S.; Krokidis, X.; Fuster, F.; Silvi, B. *Comput. Chem. (Oxford)* **1999**, *23*, 597.
(39) (a) Laaksonen, L. *J. Mol. Graphics* **1992**, *10*, 33. (b) Bergman, D. L.; Laaksonen, L.; Laaksonen, A. *J. Mol. Graphics Modell.* **1997**, *15*, 301.
(40) Reed, A. E.; Curtiss, L. A.; Weinhold, F. *Chem. Rev.* **1988**, *88*, 899.
(41) Perdew, J. P.; Chevary, J. A.; Vosko, S. H.; Jackson, K. A.; Pederson, M. R.; Singh, D. J.; Fiolhais, C. *Phys. Rev. B* **1992**, *46*, 6671.
(42) Clark, T.; Chandrasekhar, J.; Spitznagel, G. W.; Schleyer, P. v. R. *J. Comput. Chem.* **1983**, *4*, 294.
(43) Tai, T. B.; Grant, D. J.; Nguyen, M. T.; Dixon, D. A. *J. Phys. Chem. A* **2010**, *114*, 994.
(44) Zhai, H. J.; Wang, L. S.; Zubarev, D. Y.; Boldyrev, A. I. *J. Phys. Chem. A* **2006**, *110*, 1689.
(45) Boldyrev, A. I.; Wang, L. S. *Chem. Rev.* **2005**, *105*, 3716.
(46) Santos, J. C.; Tiznado, W.; Contreras, R.; Fuentealba, P. *J. Chem. Phys.* **2004**, *120*, 1670.
(47) Poater, J.; Duran, M.; Sola, M.; Silvi, B. *Chem. Rev.* **2005**, *105*, 3911.
(48) Lipscomb, W. N. *Boron Hydrides*; W. A. Benjamin: New York, 1963.
(49) Dewar, M. J. S.; Deal Lano, C. *J. Am. Chem. Soc.* **1969**, *91*, 789.
(50) Zhan, C. G.; Zheng, F.; Dixon, D. A. *J. Am. Chem. Soc.* **2002**, *124*, 14795.
(51) Doering, W. von E.; Beasley, G. H. *Tetrahedron* **1973**, *15*, 2231.
(52) Benson, S. W. *Thermochemical Kinetics*; John Wiley & Sons: New York, 1968.

JP909512M